# Spatial Distribution of Radionuclides and Their Radiation Exposure Concerning Health Impacts in the Riverbed Sediment of Dharla River of Northern Bangladesh

**Course Code: ENV 4205**

**A Thesis Submitted to the Department of Environmental Science, Faculty of Science and Technology, Bangladesh University of Professionals for Partial Fulfilment of the Requirements for the Degree of BSc in Environmental Science**

**Submitted by:**

Mithila Farzana

ID: 2053201019

Department of Environmental Science

Bangladesh University of Professionals (BUP)

**Submitted to:**

**Supervisor**

Dr. Md. Mostafizur Rahman

Associate Professor,

Department of Environmental Science

Jahangirnagar University, Dhaka

Adjunct Faculty

Bangladesh University of Professionals

(BUP)

**December 2023**

**DEDICATED TO**

**My Family, friends and my respected seniors who's support and guidance motivated and helped me accomplish my thesis**

**And**

**All of my respected supervisors, who actively guided and supported me**

## ACKNOWLEDGEMENTS

All praises to Allah, the benevolent and the merciful.

I want to express my gratitude to those who have supported me throughout my entire BSc and played a role in the completion of this thesis. This work would not have been achievable without their assistance.

I would like to thank my wonderful thesis advisor and instructor, Dr. Md. Mostafizur Rahman Associate Professor, Environmental science department, Jahangirnagar University and adjunct faculty, Environmental Science, Bangladesh University of Professionals (BUP). His steadfast assistance and direction were crucial to the completion of this study and the writing of this extensive paper. I can never thank him enough for his contributions. I was inspired by him every time and I worked hard to finish this research so that I might become more adept at addressing problems. This thesis paper would never have been completed without his constant supervision.

My sincere appreciation goes out to my co-supervisor, Dr. Rahat Khan, who serves as the Principal Scientific Officer of the Institute of Nuclear Science and Technology (INST), Atomic Energy Research Establishment (AERE), Reactor and Neutron Physics Division (RNPD). Throughout my study, his unwavering direction, close supervision, continuous encouragement, astute counsel and efficient oversight were invaluable. My knowledge and abilities were much increased by this educational experience, enabling me to make a big contribution to my country.

Lastly, I must express my gratitude to my parents, my friends and respected seniors for their unwavering mental support, collaboration, and constant encouragement.

## DECLARATION

I hereby declare that the research work entitled " **Spatial Distribution of Radionuclides and Their Radiation exposure Concerning Health Impacts in the Riverbed Sediment of Dharla River of Northern Bangladesh**" has been carried out under the Department of Environmental Science, Faculty of Science and Technology, Bangladesh University of Professionals for the fulfilment of the BSc in Environmental Science degree requirement. I have used my own laboratory analyses to obtain original research findings for this thesis, which I have supplemented with references from existing literature. This work has not been submitted for credit towards another degree at any other university, either in full or in part. In addition, I certify that this thesis contains no plagiarized material (Maximum 25%).

25/11/2023

Name: Mithila Farzana
Roll No.: 2053201019
Registration No.:102001200019
Session: 2019-2020
Department of Environmental Science
Faculty of Science and Technology
Bangladesh University of Professionals

## CERTIFICATE OF THE SUPERVISOR

This is to certify that Mithila Farzana carried out her thesis under my supervision and guidelines and prepared the thesis entitled " Spatial Distribution of Radionuclides in the Riverbed Sediment of Dharla River of Northern Bengal". To the best of my knowledge, the materials and sources from other researchers that were used in this work have been duly acknowledged by the author. Additionally, the thesis has not been submitted to any other university or institution in order to receive a different degree or credential.

Therefore, it is suggested that the thesis be presented to the Department of Environmental Science, Faculty of Science and Technology, Bangladesh University of Professionals, to meet the criteria for the conferment of the BSc in Environmental Science degree. I also confirm the absence of any plagiarized content in this thesis.

25/11/2023

.....

**Supervisor**
Dr. Md. Mostafizur Rahman
Associate Professor,
Department of Environmental Science
Jahangirnagar University, Dhaka
Adjunct Faculty

Bangladesh University of Professionals
(BUP)

# Abstract

In order to study the geogenic processes affecting naturally occurring radioactive materials (NORMs: $^{226}Ra$, $^{232}Th$, $^{40}K$) distribution, the trans boundary Himalayan River Dharla is chosen, which has little evidence of human influence. Heavy metals like lead (Pb), titanium (Ti), actinium (Ac), bismuth (Bi), cesium (Cs) and potassium (K) are investigated with 30 riverbed sediment samples taken from 10 different locations of the Dharla River in Bangladesh. The elemental abundances and NORM activity were measured by neutron activation analysis (INAA) and HPGe Gamma-Spectrometry, respectively. Using the Triga Mark II research reactor to irradiate the sample, INAA uses gamma spectrometry to operate. The wide range of applications and non-invasive nature of INAA make it the preferred option. The findings shed light on the naturally occurring radioactivity levels in the riverbed silt, which is important knowledge for comprehending the dynamics of the local environment and geology. In order to appraise the quality of irradiation and the precision of the findings, the analysis also involves evaluating standard soils and sediment samples placed among the samples that were collected. The concentration of these components is then carefully examined using a variety of computations and patterns to describe the level of contamination and pollution in the region. The information gathered is mainly used to calculate the Radium equivalent activity ($Ra_{eq}$), External hazard index ($H_{ex}$), Internal hazard index ($H_{in}$), Absorbed dose rate (D), Annual effective dose rate ($E_{aed}$), Gamma representative level index ($I_{\gamma}$), Activity utilization index (AUI) and Excess lifetime cancer risk (ELCR) which provide a broad picture of the level of pollution in river sediments. Compared to matching global mean values, the average radioactivity concentrations of $^{226}Ra$ (60.7 $Bq.kg^{-1}$), $^{232}Th$ (40.5 $Bq.kg^{-1}$), and $^{40}K$ (663 $Bq.kg^{-1}$) were 1.0-1.05 times higher. Radiological indices suggested possible long-term health effects, while GeoEnvironmental indices revealed chemical element concentration in heavy minerals. This study advances our knowledge of radionuclide behaviour in riverine ecosystems and has practical applications in risk assessment and environmental management.

**Keywords**

*Dharla, INAA, HPGe, Gamma-Spectrometry, Naturally Occurring Radioactive Materials (NORM), Radium equivalent activity, Trans boundary, Ionising- radiation, Interference, Excess lifetime cancer risk (ELCR)*

# List Of Tables



| Serial No. | Name of Table | Page No. |
|---|---|---|
| 01. | Table 3.1 The sample collection information is presented in the following | 40 |
| 02. | Table 3.2 Weight of the sample and poly bag/pot | 44 |
| 03. | Table 3.3 Radionuclides' Lower Limit of Detection (Khan et al., 2021) | 52 |
| 04. | Table 3.4 Short Irradiation Criteria of 3 MW TRIGA MARK-II reactor | 55 |
| 05. | Table 3.5 Long Irradiation Criteria of 3 MW TRIGA MARK-II reactor | 55 |
| 06. | Table 5.1 A comparison of activity concentrations of $^{226}Ra$, $^{232}Th$ and $^{40}K$ radionuclides (in $Bqkg^{-1}$) and the radiological | 64 |

| | | |
|---|---|---|
| | indices associated from this study with the literature data on Dharla River | |

# List of Figures


| Serial No. | Name of Figures | Page No. |
|---|---|---|
| 01. | Figure 2.1 Process of reviewing the pre-existing literature | 26 |
| 02. | Figure 3.1 A flowchart of methodology adopted for the study | 38 |
| 03. | Figure 3.2 Location of the study area showing specific location of sampling in the Dharla river of northern Bangladesh. | 39 |
| 04. | Figure 3.3 Sample drying in micro-oven | 42 |
| 05. | Figure 3.4 Sieving of the soil sample | 42 |
| 06. | Figure 3.5 Grinding of the samples | 43 |
| 07. | Figure 3.6 Digital electronic microbalance and thermal sealer | 44 |
| 08. | Figure 3.7 Prepared samples | 46 |
| 09. | Figure: 3.8 The flow chart of soil sample preparation | 46 |
| 10. | Figure 3.9 Block diagram of gamma ray detector setup | 47 |
| 11. | Figure 3.10 HPGe detector system in BAEC, Savar, Dhaka | 48 |
| 12. | Figure 3.11 Cross- sectional view of HPGe detector (Khan et al., 2021) | 49 |

| | | |
|---|---|---|
| 13. | Figure 3.12 The typical correlation between the channel number of gamma rays and their observed energies during energy calibration. | 50 |
| 14. | Figure 3.12 The typical correlation between the channel number of gamma rays and their observed energies during energy calibration. | 51 |
| 15. | Figure 3.14 Block Diagram of the gamma ray detection | 53 |
| 16. | Figure 3.15 Sending and receiving centre for sample vial in BAEC, Savar | 56 |
| 17. | Figure 3.16 Gamma peak analysis with Hypermet PC (5.12) | 57 |
| 18. | Figure 3.17 Graphical presentation of accuracy and precision | 58 |
| 19. | Figure 5.1 Radium Equivalent Activity ($R_{aeq}$) | 74 |
| 20. | Figure 5.2 External Hazard Index ($H_{ex}$) | 75 |
| 21. | Figure 5.3 Internal Hazard Index ($H_{in}$) | 75 |
| 22. | Figure 5.4 Annual effective dose rate ($E_{aed}$) | 76 |
| 23. | Figure 5.5 Gamma representative level index ($I\gamma$) | 77 |
| 24. | Figure 5.6 Activity utilization index (AUI) | 77 |
| 25. | Figure 5.7 Excess lifetime cancer risk (ELCR) | 78 |
| 26. | Figure 5.8 Spatial distribution of radionuclides in the riverbed sediment of Dharla river. | 84 |

# Abbreviations

| Abbreviations | Full forms |
|---|---|
| AAS | Atomic Absorption Spectrometry |
| ADC | Analog to Digital Converter |
| AERE | Atomic Energy Research Establishment |
| DIM | Detector Interface Module |
| IAEA | International Atomic Energy Agency |
| ICP-AES | Inductively Coupled Plasma Atomic Emission Spectrometry |
| ICP-MS | Inductively Coupled Plasma Mass Spectrometry |
| ICP-OES | Inductively Coupled Plasma Optical Emission Spectrometry |
| MCA | Multi-Channel Analyser |

# Table of Contents

Abstract ..... 6

List Of Tables ..... 7

List of Figures ..... 8

Abbreviations ..... 10

Chapter 01 ..... 14

Introduction ..... 14

1.1 Background of the study ..... 15

1.2 Problem statement ..... 16

1.3 Rationale of the study ..... 17

1.4 Research Questions ..... 18

1.5 Research Hypothesis ..... 19

1.6 Objectives of the study ..... 19

1.7 Limitations of the Study ..... 19

1.8 Explanation of Important Terms Used ..... 20

1.9 Outline of the thesis ..... 22

Chapter 02 ..... 24

Literature review ..... 24

2.1 Review of existing literature ..... 26

2.2 Research Gap Analysis ..... 35

Chapter 03 ..... 36

Methods and Methodology ..... 36

3.1 Research Design ..... 37
3.2 Study Area Location ..... 39
3.3 Sample Collection Procedures ..... 40
3.4 Steps of Sample Preparation ..... 41
3.4.1 Drying ..... 41
3.4.2 Sieving ..... 42
3.4.3 Grinding ..... 43
3.4.4 Weighing ..... 43
3.5 Preparation of Sample for HPGe Detector ..... 45
3.6 Setup of the experiment ..... 47
3.6.1 High Purity Germanium detector (HPGe) ..... 47
3.6.2 Standard Gamma Ray sources ..... 49
3.6.3 Detector Parameters Calibration ..... 49
3.6.4 HPGe Detector Efficiency Calibration ..... 51
3.6.5 Lower Limit of Detection (LLD) of Radionuclides ..... 52
3.6.6 Gamma Ray Detection ..... 52
3.7 Preparation of sample for INAA ..... 53
3.8 Experimental setup for INAA ..... 54
3.8.1 Application of INAA ..... 54
3.8.2 Irradiation ..... 54
3.8.3 Gamma Ray Counting ..... 56
3.8.4 Concentration Calculation ..... 57
3.8.5 Accuracy and Precisions ..... 58
3.9 Secondary data sources ..... 58
Chapter 04 ..... 59
Data Analysis ..... 59

4.1 Various Radiological and Environmental Indicators ..... 60
4.1.1 Raeq or Radium equivalent activity ..... 60
4.1.2 External hazard index (Hex) and Internal hazard index (Hin) ..... 60
4.1.3 Absorbed dose rate (D) ..... 60
4.1.4 Eaed or Annual effective dose rate ..... 61
4.1.5 Gamma representative level index (Iγ) ..... 61
4.1.6 Activity utilization index (AUI) ..... 61
4.1.7 Excess lifetime cancer risk (ELCR) ..... 61
4.2 Statistical analysis ..... 62
Chapter 05 ..... 63
Result and Discussion ..... 63
5.1 Statistical analysis result of occurrence and NORMs distribution ..... 64
5.2 Radiological Risk ..... 73
5.3 Policy Implications ..... 76
Chapter 06 ..... 82
Conclusion ..... 82
Chapter 08 ..... 84
References ..... 84

# Chapter 01

# Introduction

## 1.1 Background of the study

The Earth formed from a mixture of dust and gas encircling the early sun more than 4.6 billion years ago. It grew as a result of several collisions between dust grains, asteroids, and newly formed planets (Warren, n.d.). With the course of time the structure of the earth was modified through various geological and atmospheric incidents and changes. In these terms, the various geological incidents like earthquakes and volcanic eruptions have been the reasons behind the present geological condition of the earth and also various natural radioactivity in the soil of different places (*Volcanos and Radioactivity on JSTOR*, n.d.). Located at the meeting point of the Eurasian, Indian, and Burmese plates, the Bengal Basin is a collisional foreland basin in South Asia that stretches into parts of Bangladesh and the Indian states of West Bengal, Tripura, and Assam according to Hossain et al. (2019). As the Bengal region was formed from the collective decomposition of various sediments coming from different location of the Himalayan transboundary rivers as observed by Rashid, (2022), these rivers also carry many natural radionuclides according to Khan et al. (2023).

Ionising radiation exposure in river sediments comes from a variety of sources, such as radionuclides from the decay series of $^{238}U$ and $^{232}Th$ present in soil, rocks as well as cosmic radiation from the Earth's outer atmosphere and naturally occurring terrestrial sources such gamma rays released by $^{40}K$ according to Azeem et al. (2023). In addition, man-made activities such as nuclear treatment, weapon testing, accidents, and the nuclear power cycle contribute to the environmental contamination of artificial radioisotopes. The degree of exposure to both natural and extra-terrestrial radiation varies and is impacted by regional variations in geological and radiochemical characteristics.

The internal structures of unstable or radioactive molecules are the source of ionising radiation. The excess internal energy in these atoms' nuclei causes spontaneous modifications that release more energy in the form of beta, gamma, or alpha particles—a condition known as radioactivity. Globally, there are differences in the amounts of natural ambient radioactivity and exogenous exposure to gamma radiation due to regional geological and geographical factors (UNSCEAR, 2000).

Despite the fact that radiation is inevitable in environmental materials, there is a growing global concern about its possible effects on human health (UNSCEAR, 2000; 2010). The presence of

radioactive elements that occur naturally such as Th, U, and their derivatives, as well as K-40, in natural geomaterials has led to a plethora of research on natural radioactivity worldwide. It is essential to monitor radioactive elements for the preservation of the environment, human health, and living things. As a result, quick and precise techniques for determining radioactivity are desperately needed insisted by El-Bahi (2004).

## 1.2 Problem statement

According to El Samad et al. (2013), artificial radionuclides created by human activity and naturally occurring radioactive materials (NORMs) expose living things to a wide range of ionising radiations on a regular basis. The Earth's environment contains naturally occurring radioactivity from NORMs in a variety of geological formations, including soils, minerals, water, sediments, air, and building materials. Among other things, nuclear weapon testing, incidents involving nuclear weapons, and industrial and medical uses are the sources of artificial radionuclides. The natural radioactive isotopes of $^{238}U$, $^{232}Th$, and their daughter products, as well as $^{40}K$, account for over 87% of the radiation doses that people are exposed to (Shetty & Narayana, 2010; UNSCEAR, 1993). Two notable radionuclides, $^{226}Ra$ and $^{228}Ra$, decay to produce other radionuclides. Sediment not only provides a substantial source of exposure to radiation for aquatic life, but it also acts as a conduit for radionuclide movement in aquatic environments.

Both internal radiation from inhalation and exterior radiation from radiation originating specifically from primordial radionuclides in sediments are two ways that sediment adds to human radiation exposure. The latter mostly affects the lungs because of radon and its breakdown products that come from construction materials, soil, and sediment. Long-term radioactive exposure and radionuclide inhalation can have serious health effects, such as leukaemia and chronic lung cancer. Researchers Jibiri & Okeyode (2012), Ngachin et al. (2007), Hameed et al. (2014), and Qureshi et al. (2014) have all explored this material.

Sand and gravel are commonly found in the material that builds up at the bottom of rivers and lakes, making them a very useful resource for construction projects. River sediments are used widely as basic building materials in Bangladesh, especially those from the Dharla River. Because the public continues to use these sediments as vital building materials, it is imperative that the

concentrations of activity of natural radionuclides found in these sediments be carefully analysed in order to assess the potential dangers to radiological health.

## 1.3 Rationale of the study

$Ra_{eq}$ values generally show stability when compared across regions which have comparable geological conditions and are unaffected by geological or human influences according to Islam et al. (2019) and Khan et al. (2019). As such, notable fluctuations in $Ra_{eq}$ values seen during the evaluation of radium equivalent activity in particular sites may indicate modifications to the unique behaviours of NORM as a result of geological or human activities.

Geological elements like rock type, geographical parameters like location and altitude, and mineralogical characteristics like soil and rock composition all have a significant impact on natural radioactivity and the exposure to gamma radiation (from radionuclides) as assessed by Ahad et al. (2004). Thorium and uranium are the elements that contribute to radioactivity in naturally occurring radioactive materials (NORMs), which include minerals such as zircon, ilmenite, rutile, xenotime, and monazite (IAEA, 2004).

Fertilisers with heavy metals and NORMs, especially phosphate-based fertilisers including uranium, release these components into the surroundings in agricultural regions around the world according to Milica et al. (2012). Approximately 73% of all ambient uranium comes from fertiliser use, making it a substantial generated by humans found by Stojanovi et al. through his research in 2012. Radionuclide particles from these kinds of sources are more likely to be globally dispersed through air currents and end up on Earth's surface if they are linked with heavy and persistent precipitation. This mechanism makes it possible for radioactive materials to get into the food chain, water supply, and atmosphere.

The pervasive heavy metal pollution of aquatic habitats is clearly a global concern. Sediment-focused scientific research offers vital information for comprehending how human activity affects these ecosystems according to a study by Sayadi et al. (2010). While contamination with heavy metals in sediment has been assessed in rivers all over the world, Bangladesh—and especially the northern Dharla River—has not gotten much attention in prior studies. Studies on heavy metal pollution in the Dharla River are conspicuously lacking, which creates a knowledge vacuum about

the dispersion of radioactive elements within the silt. The river provides an important source of water for agriculture, sustains a variety of fish populations, and is essential to the maintenance of livelihoods.

In addition, the Dharla River facilitates the dispersal and deposition of significant pollutant loads from a variety of sources. The causes of heavy metal pollution include untreated domestic effluent mixed with improperly disposed of solid waste, fast population growth, improper planning for residential developments in the catchment area, industrial and medical waste discharge, agricultural runoff, sporting events, and the discharge of poultry waste. As such, pollution levels in the river's sediment and water may be ten times greater than in pre-industrial periods. It becomes essential to identify heavy metal contamination and do NORM analysis in order to assess the harmful effects it has on aquatic ecosystems.

This study could be useful for institutional management as well as environmental monitoring organisations since it compares the level of radioactivity and the number and amount of heavy metals released by the studied river with data from the literature. It could be useful for creating and managing policies for legislators and senior government officials.

## 1.4 Research Questions

Taking into account the research challenges and significant gaps in previous studies, the following primary research questions are formulated:

1. What are the natural radionuclide concentrations in the Dharla River sediment ($^{226}$Ra, $^{232}$Th, and $^{40}$K)?

2. What is the concentration of elements in the Dharla River basin?

3. How are the natural radioactivity levels and study metal distributions distributed geographically in the Dharla River sediments described?

4. Based on radiation health hazard indices (ELCR), what health hazards do locals and tourists have from naturally occurring radionuclides (such as $^{40}$K, $^{232}$Th, and $^{226}$Ra)?

5. What may be deduced about the degree of contamination and pollution in the Dharla River from an evaluation of elemental abundances?

## 1.5 Research Hypothesis

The study's hypothesis was that, in comparison to other trans boundary rivers, the Dharla River basin was less affected by human activity. As such, it was considered a suitable site for carrying out an evaluation of combined elemental as well as NORM analysis.

## 1.6 Objectives of the study

In order to ascertain the trans boundary river Dharla's inclination or declination with respect to other rivers, the primary objective of this study is to determine the concentration of naturally occurring radioactive materials, such as $^{226}Ra$, $^{232}Th$, and $^{40}K$.

The objectives of the study are as follows:

- To observe baseline data on radionuclides found in the Dharla River naturally.
- To determine the chemical composition of the Dharla riverbed sediment samples that are collected by INAA.
- To investigate the distribution of naturally occurring radioactivity in the sediments of the Dharla River.
- To evaluate the radiation health hazard status and the degree of contamination and assess the health risks posed by naturally occurring radiation.
- To evaluate the excess lifetime cancer risk (ELCR) and the radiation-related health hazards indexes in the assigned study region and understand their effects on human health.

## 1.7 Limitations of the Study

All experiments and research projects have limits by nature. Notwithstanding these limitations and the recognition of study gaps, it is possible to overcome and handle these obstacles in subsequent

studies, which would increase the research's usefulness. The following lists a few of this study's limitations:

- While the use of High-Purity Germanium (HPGe) and Instrumental Neutron Activation Analysis (INAA) in this study is decisive for identifying elemental and NORM composition, it also includes the handling of radioactive samples, requiring careful handling and disposal protocols. Furthermore, interference might cause differences in the detection accuracy for distinct elements, necessitating a large amount of data for analysis.
- The baseline data used in this study for comparisons is not a universal example, but rather a relative one. Various background data sets, including the upper crust of the continent, may be used in other investigations based on the feasibility of the work and the accessibility of the data.
- The data used is only subjected to a single season and it may vary based on the sediment flows in various seasons.

As a result, our analysis emphasises the need for more research because it is unable to give a thorough picture of the dangers associated with geology and radioactivity.

## 1.8 Explanation of Important Terms Used

- **$R_{aeq}$ or Radium equivalent activity** - A common metric for assessing the radiological dangers connected to radioactivity in environmental materials is radium equivalent activity. $Ra_{eq}$ is used to determine the effective equivalent dose rate (Tufail, 2012).
- **External hazard index ($H_{ex}$)** - Beretka and Mathew developed the external hazard ($H_{ex}$) index, which is an additional radiation hazard index used to evaluate the rate of indoor radiation exposure from external exposure to gamma radiation emitted by naturally occurring radionuclides found in residential building materials (J. Beretka & P. J. Mathew, 1985).
- **Internal hazard index ($H_{in}$)** - Analyse the rate at which gamma radiation from naturally occurring radionuclides present in residential building materials is exposed internally (Mbonu & Ben, 2021).

- **Absorbed dose rate (D)** - The amount of energy that is ionising radiation transfers to matter per unit mass is measured by a metric called absorption dose (Windsor & Michaels, 2007).
- **$E_{aed}$ or Annual effective dose rate** - Within the framework for radioactive protection developed by the International Commission on Radioactive Protection (ICRP), effective dose is one of the dosage metrics. It allows the aggregation of organ doses from various amounts and types of radiation, both internal and external, to calculate an all-inclusive effective dose. It does this by taking into account the type of radiation and the properties of each organ or tissue absorbing radiation (Boumala et al., 2019)
- **Gamma representative level index ($I_\gamma$)** - The European Commission's radiation hazard index, or $I_\gamma$, can be used to estimate the risk of gamma radiation, especially when dealing with naturally occurring radionuclides (Bavarnegin et al., 2013).
- **Activity utilization index (AUI)** - It is utilized to estimate the sum of radionuclides in soil (Joel et al., 2019).
- **Excess lifetime cancer risk (ELCR)** - Determines the potential of any element to cause cancer (Qureshi et al., 2014).
- **REE** - According to the International Atomic Energy Agency (IUPAC), a rare-earth element (REE) is any of the seventeen chemical elements found in the periodic table, which also includes the fifteen lanthanides, scandium, and yttrium. Because of their similar chemical properties and presence in the same ore sources as lanthanides, yttrium and scandium are regarded as rare-earth elements.
- **HPGe** - The High Purity Germanium detector (HPGe) is the only radiation detection tool that offers enough data to identify radionuclides with accuracy and dependability using only their passive gamma-ray emissions.
- **Instrumental Neutron Activation Analysis (INAA)** - This technique is used to examine a wide variety of matrices for the presence of major and trace elements.
- **$I_{geo}$** - Müller's geo-accumulation index ($I_{geo}$), which was developed in 1969, makes it easier to evaluate environmental pollution by contrasting concentrations from pre-industrial times with present ones.

- **Principal Component Analysis (PCA)** - PCA is a widely used method to reduce the dimensionality of large-scale data sets by distilling a large number of variables within a smaller set that preserves the majority of the information.
- **Pearson Correlation** - Because of its covariance principle, Pearson's correlation coefficient evaluates the statistical link between two dependent variables and is regarded as the most effective method for establishing a relationship between variables.
- **CD** - The Contamination Factor (CF) can be used to assess the Degree of Contamination (CD), which represents the total impact of water-quality indicators that are considered hazardous for household water use (Blackman et al., 1997).
- **Upper Continental Crust (UCC)** - The continent's upper crust, which is the easiest to reach, has a limited composition and acts as a benchmark.
- **Spatial Distribution** - A way to arrange or show geographic data that illustrates how a phenomenon behaves.
- **Geographic Information System (GIS)** - This system links location data with descriptive data for visualisation and evaluation purposes in research and diverse businesses. It generates, manages, analyses, and maps different types of data.

## 1.9 Outline of the thesis

The next chapters of the thesis follow the following order:

**Chapter 02**: This chapter includes the literature review and includes

- Analysis of existing literature
- Their major findings and
- The research gap from those

**Chapter 03**: The chapter includes the methods and methodology part and discusses

- Research design
- Study area

- Method of sample collection
- Sample preparation
- Method of experiment
- Sources of data collection

**Chapter 04**: This chapter includes data analysis, discussing

- Obtained data are analysed through various indexes
- The data and their relation are shown through statistical and spatial approaches

**Chapter 05**: The chapter includes the results and their discussion and objects to

- Discuss how the result varies from the initial hypothesis
- How the naturally occurring radionuclides affect human health

**Chapter 06**: This chapter sums up a conclusion regarding all the data and the findings.

The ending part of the report includes references, appendix section and any supplementary used in the research.

# Chapter 02

# Literature review

Ionising radiation from radioactive elements, both naturally occurring and man-made, is a constant threat to the biosphere of the Earth. It affects all living things. Radiation exposures of various kinds are widespread across the world, and they are influenced by human activity. As such, it is imperative to examine the radiation concentrations found in various natural environmental components.

This study's main goal was to determine whether naturally occurring radionuclides and pollution levels were present in the Dharla River silt. Many places in the world, including Bangladesh, have had studies done on radionuclide concentrations in soil and water, which have shed light on pollution levels and the existence of radioactivity in various nations. A survey of the literature was done, and new issues of noteworthy journals with pertinent content were assessed.

The Dharla River is located in a rural area of northern Bangladesh and lacks sources of industrial and urban pollution, it is expected to show less anthropogenic discharge. The river has been the subject of few studies that have examined topics like the fragility of wetland habitats, the damming effect, and the effects of changed flow on active inundation zones. These studies have prepared the ground for future research into ecological issues and environmental imbalances brought on by the persistent presence of heavy metals in the river's sediment.

A diagram is given as follows to portray the process of reviewing literature for the research.

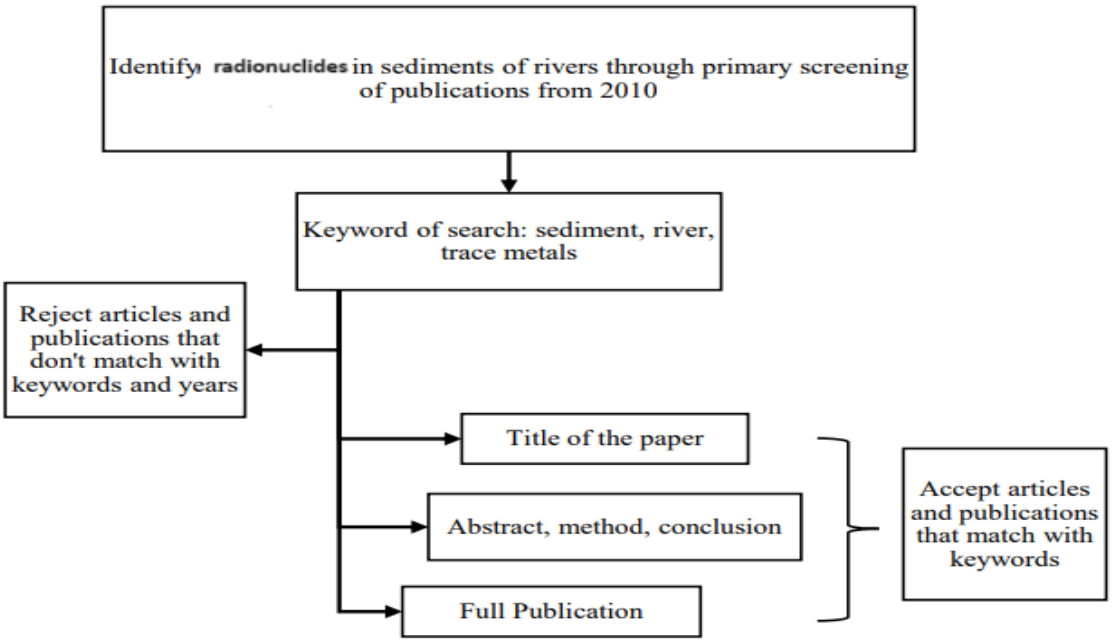


**Figure 2.1 Process of reviewing the pre-existing literature**

## 2.1 Review of existing literature

Using the Hakanson Risk Index and Monte Carlo Simulation techniques, **Acharjee et al. (2022)** conducted a future ecological risk index analysis to examine heavy metal contamination in the Surma River. A concentration pattern of specific heavy metals in the area was found by the investigation, including Ni > PC > Mn > Cu > Zn. There was no evidence of serious sediment pollution, with the exception of Ni. The results of the Monte Carlo Simulation and danger Index both pointed to a minimal ecological danger from the heavy metals that were studied, providing important information on the pollution profiles of rivers and the susceptibility of sediment in rivers close to urban areas to heavy metal pollution.

The Teesta River in Bangladesh has higher radioactivity than other freshwater basins in the globe, according to **Khan et al. (2021)**. We used instrumental neutron activation analysis (INAA) and gamma spectrometry to determine elemental abundances and naturally occurring radionuclides in the sediment samples. An extensive study of the enhanced radioactivity, concentrating on the

compositional elements of heavy minerals, was spurred by the finding that the amounts of rare earth elements were twice as high as those found in the crust. The presence of heavy minerals, especially monazite, was confirmed by statistical analysis and enrichment of light rare earth elements. Hydrodynamic forces in rivers carry suspended sediments through a complex process of transit, filtration, and recycling. The preponderance of felsic-source components over mafic components was confirmed by elemental ratios.

**Islam et al. (2015)** assessed the ecological dangers and heavy metal concentrations in surface sediment of Bangladesh's Buriganga River. Indicators like the enrichment factor (EF), contamination element (CE), and pollution load index (PLI) were used in the assessment. With all research locations exhibiting moderate to severe heavy metal toxicity based on total toxic units (PTUs), the mean PLI value suggested that metal toxicity was contributing to the deterioration of the sediment. For the sediments in the Buriganga River, potential ecological risk evaluations varied from high to very high.

**Ali et al. (2019)** examined hazardous elements such as arsenic, chromium, cadmium, and lead with a focus on Bangladesh's Pasur River. The results of the investigation showed that the higher metal concentrations in the water from this river exceeded the standards for safe drinking water. Sediment deterioration was shown to be rising over time, according to ecological risk assessments, including PLI. The Cd contamination factor (CF) values demonstrated the substantial influence of Cd on the sediments under investigation, even if environmental degradation was determined to be mild to moderate.

**Islam et al. (2020)** examined metalloids and heavy metals in Bangladesh's Halda River water and sediments. As, Cd, and Pb contents in sediments were higher than those in reference levels. The Halda River sediments showed moderate to high levels of Cd contamination and low to moderate levels of As and Pb contamination, according to pollution indexes. Multivariate research found that just four metals—lead, zinc, cadmium, and chromium—originate from natural geogenic processes, placing cadmium as a moderate to severe danger to ecosystems.

On the other hand, **Kormokar et al. (2019)** investigated the ecological impacts of heavy metal pollution in the Louhajong River. Wintertime sediment levels of measured metals, geo-accumulation indices, contamination factors, and pollutant load indices were higher than summertime levels, according to indicators such as the enrichment factor (EF). According to

ecological concern, the pollutants were ordered as follows: As > Cu > Cd > Ni > Pb > Cr. The sediments showed little toxicity to heavy metals.

Using Atomic Absorption Spectrophotometry (AAS), **Siddique et al. (2021)** examined sediment samples from the Meghna River estuary to assess the levels of six heavy metal pollution. The lower Meghna River estuary showed no signs of Fe, Zn, Pb, Cr, or Cu according to geo-accumulation, contamination, and pollution load indices. Between Fe and Pb, a substantial Pearson correlation coefficient was found, suggesting little to no effect on the metal distribution pattern.

**Islam et al. (2017)** evaluated 16 trace elements in sediments of the Sundarbans mangrove forest Rivers in the wake of an oil leak in the Sela River of the Sundarbans. There were reports of elevated amounts of V, Cr, Fe, and Cd; As, Sb, Th, and U showed moderate levels of pollution, while Cd showed moderate to severe levels of pollution. Potential ecological impact from exposure to elevated amounts of Cr, Ni, Cu, and As was revealed by multivariate statistical analysis.

**Das et al. (2016)** looked into the existence and fate of trace elements in bottom sediments from the Karnaphuli River. The total amounts of 15 major and trace elements were ascertained by neutron activation analysis (INAA). Al, Ti, V, Zn, and Rb concentrations in sediments were greater than those in the upper continental crust (UCC). Pollution indices showed that core sediments have more contaminants than originally thought.

In order to evaluate the risks heavy metals (HMs) cause to the environment and public health in the Vatukoula Goldmine region (VGR) of Fiji, **Kumar et al. (2022)** used a multidisciplinary approach. High levels of Cd, Pb, and Zn contamination were found in sediment samples, along with a complex web of coexistence between lead and other metals like Mn and Ni. The primary sediment source patterns were found to be Cr, Cd-Pb, Mn, and Zn, according to source apportionment and principal component analysis. Particularly in youngsters, elevated levels of Cd, Pb, and Cr have been linked to major health impacts that are both carcinogenic and non-carcinogenic. Significant ecological concerns were raised by the moderate to extremely contaminated circumstances around the Toko dam, and a 75% chance of hurting aquatic life was posed by the amounts of Pb and Cd near the VGR.

**Tunca et al. (2017)** used flame atomic absorption spectrophotometry and graphite furnace atomic absorption spectrophotometry (FAAS) to investigate sediment from Turkey's Aegean Sea for metal

pollution. Even with elevated Pb, Mn, As, Cd, and Cr concentrations, the enrichment factor (EF) suggested a negligible human impact. This conclusion was corroborated by the geo-accumulation index ($I_{geo}$), which showed small impact ranges and concentrations over the threshold effect level (TEL) in some areas. Attention should be paid to the stations at Ayvalk, Edremit, and Yeniköy, especially with reference to As and Ni.

**Maftei et al. (2019)** evaluated the Tazlau River in Romania for pollution and potential environmental impact caused by trace components. The most dangerous element among those examined was Cr found in the sediments of the Tazilu River. A correlation matrix and principal component analysis (PCA) identified important anthropogenic vs. geogenic sources, and a skin exposure assessment revealed no indication of carcinogenic or non-carcinogenic risk. Pb was a geological element, whereas Cd, Cr, and other elements mostly came from human sources.

Sediments from the North Chinese estuary in Dongying were collected by **Liu et al. (2018)**, who found that the total amounts of heavy metals decreased as follows: Cr > Zn > Cu > Pb > As > Cd > Hg. The major providers of heavy metals that are harmful to the environment are Cd and Hg, according to the potential ecological risk index (PERI), which showed low to moderate risk. Using surface sediments from 42 locations, **Gao et al. (2012)** investigated heavy metal contamination in the northwest shore of Bohai Bay, China. The concentrations of Cd, Cr, Cu, Ni, Pb, and Zn were examined; Cd was the only metal with poor mobility. A 21% toxicity risk was associated with the heavy metals, even though their current levels were lower than in certain other maritime coastal locations where they have accumulated due to human activity.

In their **2016** study, **Khalil et al**. examined the Brahmaputra (Jamuna) River in Bangladesh, identifying minerals and measuring natural radioactivity levels in the sand and silt. The identified minerals included quartz, monazite, feldspar, uranium fluoride, rutile, zircon, hematite, kyanite, and uranium arsenide. Higher amounts of $^{226}Ra$, $^{238}U$, $^{232}Th$, and $^{40}K$ were discovered compared to global norms. Potential radiation dangers were suggested by the computed absorbed dose rate and effective yearly dosage, which exceeded OECD standards.

**Isinkaye and Emelue (2015)** used gamma spectrometry to examine sediments from Oguta Lake, Nigeria, in order to determine radiological health issues related to naturally occurring radionuclides $^{226}Ra$, $^{232}Th$, and $^{40}K$. Although local concentrations were higher than the world

mean, they were still within the upper limit advised, indicating that they may be used safely as building materials.

**Qureshi et al. (2014)** computed radiation health hazard indices and excess lifetime cancer risk (ELCR) by analysing river sediments from Northern Pakistan for NORMs $^{226}$Ra, $^{232}$Th, and $^{40}$K. The Hunza, Gilgit, and Indus River sediments have concentrations above global averages, resulting in a high 3.2–3 ELCR factor.

Natural radiation levels were measured in sediment samples taken from the Ponnaiyar River in India by **Suresh et al. (2011)**. The average activity concentrations were within Indian and worldwide guidelines, notwithstanding some increased levels. The minerals that were identified included quartz, smectite, palygorskite, kaolinite, calcite, gibbsite, microcline feldspar, orthoclase feldspar, montmorillonite, and organic carbon. The calculated radiation hazard indices were below recommended levels, indicating that there was no substantial radiological threat to the population. Nevertheless, certain indices of radiation hazard were not examined.

**El-Gamal et al. (2007)** studied radionuclides $^{226}$Ra, $^{232}$Th, and $^{40}$K in particular as well as natural radioactivity in sediments of Egypt's Nile River. Numerous factors, including hydraulic structures, sediment types, geographical features, Nile water chemistry, phosphate fertiliser discharge, and the mineralogical structure of sediments, were found to have an impact on the non-uniform distribution of these radionuclides throughout the research area. Potential applications for these in building projects were indicated by the gamma activity consumption index. The 238U activities that were measured were 1.5 times more than the 232Th activity. Nevertheless, other analyses such as Radiation hazard indices (Raeq), Excess lifetime cancer risk (ELCR), and multivariate statistical techniques like frequency distribution, Pearson correlation analysis, and cluster analysis were overlooked in favour of analysing absorbed dose rates and the activity utilisation index alone.

The distribution of radionuclides in river sediments and coastal soils near Chittagong, Bangladesh, was examined by **Chowdhury et al. in 1999**. It was discovered that $^{232}$Th concentrations were greater than $^{238}$U concentrations, and that both $^{232}$Th and $^{238}$U activity in the region were higher than global mean values. Every sample has 137Cs confirmed to be present. The radon emission coefficient and exhalation rates above the global average. Nevertheless, the study did not use radiological hazard indicators other than radium equivalent activities or do multivariate statistical analysis.

In contrast, laboratory work was conducted with one or two health hazard indices by **El-Gamal et al. (2007), Suresh et al. (2011), and Khalil et al. (2016)**; however, Excess lifetime cancer risk (ELCR) was not included. Multivariate statistical analysis was used by Isinkaye and Emelue (2015) and Suresh et al. (2011) to find natural connections between samples or parameters; Qureshi et al. (2014) and El-Gamal et al. (2007) did not use multivariate statistical analysis.

The radiological threat posed by the accumulation of $^{238}U$, $^{226}Ra$, $^{232}Th$, and $^{40}K$ in geologically formed soils in northern India was calculated by **Mehra and Singh (2012)**. To find soil radioactivity, the study used γ-ray spectrometry with an HPGe detector. The average activity concentration of 40K was lower than the global average, but the concentrations of $^{238}U$, $^{226}Ra$ and $^{232}Th$ were higher. Multivariate analysis, internal and external hazard indices, and an evaluation of the excess lifetime risk of cancer were not performed in this study.

**Papp (2010)** used gamma spectrometry to analyse soil samples for radionuclides $^{238}U$, $^{226}Ra$, $^{232}Th$, and $^{40}K$ in order to examine natural radioactivity in the soils of eastern Hungarian counties. There were differences between the countries; for near-river plain areas, the activity ratio was found to be 1. However, other factors like the representative level index, excess lifetime cancer risk, radium equivalent activity concentration index, external and internal hazard indices, and multivariate statistical analysis were not included in the study, which only used the absorbed dose rate in laboratory experiments.

The radioactive dosage and concentrations in surface soil samples from Turkey's eastern and southern Marmara region were examined by **Kilic et al. (2008)**. Quantifiable levels of $^{137}Cs$, $^{238}U$, $^{226}Ra$, $^{232}Th$, and $^{40}K$ were found in soil samples. The soil samples' mean annual external dose rate of naturally occurring radionuclides was found to be within the worldwide range, and the best criteria for forecasting the concentration of $^{137}Cs$ was found to be the organic matter content. Nevertheless, the investigation turned up no proof that natural radionuclides and organic materials are related. There was no evaluation of the risk of cancer death, hazard index, or excess lifetime cancer risk.

Using gamma spectrometry, **Ajayi et al. (2007)** investigated the naturally occurring radioactivity of water from private wells in Akure, southern Nigeria. They measured the amounts of gamma-emitters $^{226}Ra$, $^{232}Th$, and $^{40}K$. The levels found in the water were more than the yearly effective dose limitations that had been set, according to the effective annual dose calculations for the

various age groups. However, the study was limited to laboratory work and the yearly effective dose rate because studies like AUI, $Ra_{eq}$, ELCR, and multivariate statistical analysis were not carried out.

To sum up, Excess lifetime cancer risk (ELCR) and external and internal hazard indices were not taken into account by **Mehra and Singh (2012), Papp (2010), Kilic et al. (2008)**, or **Ajayi et al. (2007)**, who all concentrated only on laboratory work using absorbed dose rate and radium equivalent activity concentration index. With the exception of **Kilic et al. (2008)**, they did not carry out multivariate statistical analyses such as frequency distribution or cluster analysis. Begumet al. (2022) conducted research on the redistributions of naturally occurring radioactive materials (NORMs) in the surroundings of a gas field located in Shabazpur, Bangladesh and assessed the radiological risks there. They collected the samples from environmental soil and sediment around the area, three samples from surface- soil, three sub- surface soil and three from bottom sediment of waste dump evaporation pond. Two other soil samples from nearby local canal outside the gas field boundary were also collected. In total, they analysed 18 samples for natural radioactivity by using a P- type co- axial high purity Germanium HPGe detector, followed by an analysis in a multi-channel analyser (MCA). They further analysed the Spectra acquisitions of the samples through a Spectra analysing software maestro- 32 (ORTEC) and genie – 2000 (Canberra). They used several indices for analysing the findings of the detectors, such as, radium equivalent activity and gamma- representative level index, external observed dose rate, annual effective dose rate and external and internal hazard indices. They also studied the risk of cancer using excess lifetime cancer risk theory. The findings include that the radioactivity concentrations of $^{226}$ Ra, $^{232}$ Th and $^{40}$ K in gas- well samples are 60 +- 13, 94 +- 14, 2200 +- 400 Bq $kg^{-1}$ whereas in environmental samples there 40 +- 9, 73 +- 11, 873 +- 180 Bq $kg^{-1}$, respectively. They concluded that the surface has in soil of that region consists of higher norms than the adjacent subsurface-soil.

In 2022, **Abedin and Khan** conducted research on primordial radionuclides in the dust samples from 23 educational institutions of north- eastern portion of Dhaka, Bangladesh to assess the risks caused by radioactivity. The collected samples were irradiated in irradiation-tube by thermal neutrons with a flux of 1.54 X $10^{13}$ $cm^{-2}$ $s^{-1}$ at 500KW for 2 hours in 3 MW TRIGA Mark-II reactor of BAEC, Dhaka. After undergoing a systematic decay, the irradiated materials were subjected to

γ-ray counting. A digital γ-spectrometer (ORTEC, DSPEC Jr™) was linked to an HPGe-γ-detector (CANBERRA, 40% relative efficiency, and 1.8 keV precision). The first 40 minutes of gamma-ray counting was carried out after about two days of decay, and the second three hours of gamma-ray counting was carried out after about seven days of decay. Th was recognised during the second gamma-ray counting (L2), while K and U were detected at the first gamma-ray counting (L1).

**Rashed-Nizam et al. (2014)** used gamma spectrometry to examine the radiation risks associated with man-made 137Cs and natural radioactive sources in soil samples taken from three residential clusters in Chittagong, Bangladesh. The results of the investigation showed that the concentrations of $^{226}$Ra, $^{232}$Th, and $^{40}$K were significantly lower than the global averages. The excess lifetime cancer risk (ELCR) was included in the radiation risks that the researchers calculated. The research area was deemed radiologically safe for human habitation based on the finding that all radiation risk measures, including outdoor gamma exposure rates, radiation hazard index (radium equivalent activity), and Hex, were below the prescribed levels. Although the UN Scientific Committee on the Effects of Atomic Radiation (UNSCEAR, 2000) reported that the annual effective dosage in soil, sand, and sediment samples exceeded global standards, and the average ELCR in sand samples was greater, the values remained within permissible bounds. The study also found that, although the amounts were well below those considered harmful to health, some parts of Bangladesh had air fallout containing artificial radioisotope 137Cs. Interestingly, multivariate statistical methods such cluster analysis, Pearson correlation analysis, and frequency distribution were not used in this study.

An examination of the "Distribution of radionuclides in soil samples surrounding Dhaka City" was carried out by **Miah et al. (1998)**. The study concentrated on naturally occurring radionuclides from the uranium and thorium families as well as fission products such as $^{40}$K and $^{137}$Cs. When comparing near-surface samples to deeper ones, the researchers found that the average concentration of $^{137}$Cs was higher in the former. The investigation of radiological hazard indicators, such as the Radiation Hazard Index, Activation Utilisation Index, External and Internal Hazard Index, Absorbed Dose Rate, and Excess Lifetime Cancer Risk, was not done, nor was multivariate statistical analysis.

**Sakib (2015)** examined 22 soil samples taken from Bangladesh's Habiganj district, concentrating on the distinct actions of man-made and natural radionuclides. The International Atomic Energy

Agency (IAEA) provided radioactive reference sources for the investigation, and a High Purity Germanium (HPGe) detector was used to capture experimental data accurately. Notably, the analysis found that radioactive $^{137}Cs$ were not traceable in any of the samples from the Habiganj region. In addition, Sakib found that in a variety of soil samples, the annual effective dose rates, gamma absorbed dose rates, external hazard index ($H_{ex}$), and radiological hazard related to natural and artificial radioactivity were all lower than the worldwide standard. Nevertheless, neither the excess lifetime cancer risk (ELCR) nor multivariate statistical analysis was used in the study to examine the contemporaneous behaviour of numerous random factors or to find any potential natural links between samples.

**Hossain et al. (2014)** measured the rate of absorbed gamma radiation dosage in outdoor environments by conducting a study in the northern part of Chittagong City Corporation. Tolerance thresholds for possible health hazards in outdoor environments were established by the researchers. The average outdoor absorbed dose rate was found to be 0.022 $Sv.h^{-1}$, and the computed dose equivalency was 0.22 $Sv.h^{-1}$. This number was found to be below the Bangladesh Atomic Energy Commission's dangerous 0.5 Sv.h-1 level. Nevertheless, multivariate statistical methods were not used in this investigation to evaluate the combined behaviour of many random variables or to reveal underlying links between samples, such as the assessment of Excess Lifetime Cancer Risk or the External and Internal Hazard Index.

In order to look into the contamination and distribution of trace elements in the sediment of the Karnaphuli River, **Das et al. (2018)** analysed three sediment cores. The total amounts of 15 main and trace elements (Na, Al, K, Sc, Ti, V, Cr, Mn, Fe, Co, Zn, As, Rb, Th, and U) in sediments from the Karnaphuli River were measured using neutron activation analysis (NAA). Most of the cores had average concentrations of Al, Ti, V, Zn, and Rb higher than those in the UCC. The study's pollution indicators showed that there has been a noticeable increase in pollution over time, with present sediment contamination levels being higher than historical levels.

One of the longest transboundary Himalayan rivers in the world, the Brahmaputra River in Bangladesh (China-India-Bangladesh), was the subject of an inquiry by **Khan et al. (2022).** Using HPGe-spectrophotometry and neutron activation analysis in a research reactor, the study concentrated on thirty sediment samples to analyse radioactive nuclides ($^{226}Ra$, $^{232}Th$, and $^{40}K$) and metal content, including transition metals (Fe, Ti, Sc, and V), rare earth elements (La, Ce, Eu, Sm,

Dy, Yb, and Lu), high field strength elements (Ta and Hf), and actinides (Th and U). In comparison to other freshwater basins, the study found that this region had higher radioactive concentrations. The deposition of heavy metals in this basin was aided by processes related to mineral recycling, sediment transport, and separation in upstream rivers. La/Th-Hf, La/Th-Yb, and La/V-Th-Yb are examples of bivariate graphs that show a higher contribution from felsic source rocks than from mafic source rocks. According to the radiological hazard assessment, locals may be at risk for ionising radiation-related health problems, especially if they reside in homes built with silt from the Brahmaputra River.

## 2.2 Research Gap Analysis

Research gaps and required changes are summed up as follows:

- There are no comprehensive and established procedures for assessing natural radioactivity in Dharla River silt.
- The $^{226}Ra$, $^{232}Th$, and $^{40}K$ natural radioactivity levels in sediments are being examined for the first time in this study.
- Additionally, related health risk indices, such as radiation hazard indices, absorbed dose rate, activation utilisation index, external and internal hazard indices and excess lifetime cancer risk in the Dharla River, are being investigated.
- Furthermore, it is unclear how the elements in this region of the river relate to one another and to the trace metal(oids) that correspond with them.
- However, given that no previous scientific study has examined the possible risks associated with using sand-based sediments from the bed as building materials within this cross-border river basin, there may be a research gap.

# Chapter 03

# Methods and Methodology

## 3.1 Research Design

There will be measurements of gamma radiation, utilising a low background PC multi-channel spectrometer in conjunction with a high resolution HPGe projector to determine the level of naturally occurring radioactivity found in soil samples collected from the Dharla River's sediment bed. This approach activates the component in this soil using highly energetic neutrons. When a material that has been jolted by a high-energy neutron tries to re-establish its equilibrium, it releases radioactive rays. One can ascertain whether a sample is radioactive by measuring the amount of radiation the irradiation beam produces. Instrumental Neutron Activation Analysis (INAA) is a quantitative, experimental, diagnostic, and correlative method used to examine elemental abundances.

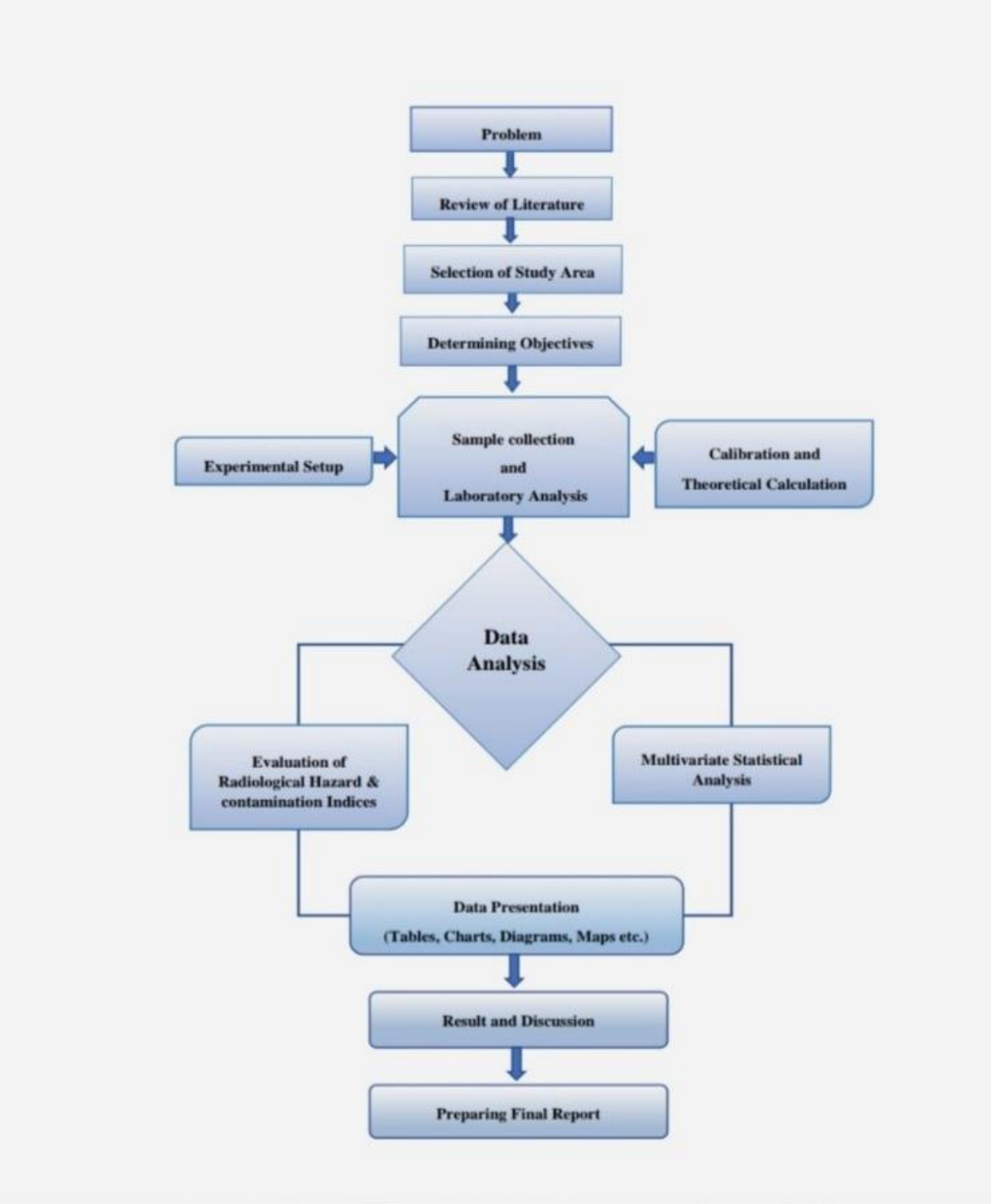


**Figure 3.1 A flowchart of methodology adopted for the study**

## 3.2 Study Area Location

The Dharla River or *Dhorola Nodi* is a tributary of the trans boundary river Brahmaputra originating from Kupup/Bitang lake of East Sikkim, Himalayas. It is flowing through India, Bhutan and Bangladesh. The river enters Bangladesh through Lalmonirhat District and unites with the Brahmaputra River near the Kurigram District. When the river approaches Patgram Upazila, it reverses its direction to the east, re-entering India. It subsequently heads southward slowly and windingly and re-enters Bangladesh through Phulbari Upazila in Kurigram District. The river's maximum depth is 39 feet (12 metres) at its point of origin in Kurigram, while its average depth is 12 feet (3.7 metres). 30 sediment samples were collected from different locations of the river's riverbed around the borders of two districts, Lalmonirhat and Phulbari.

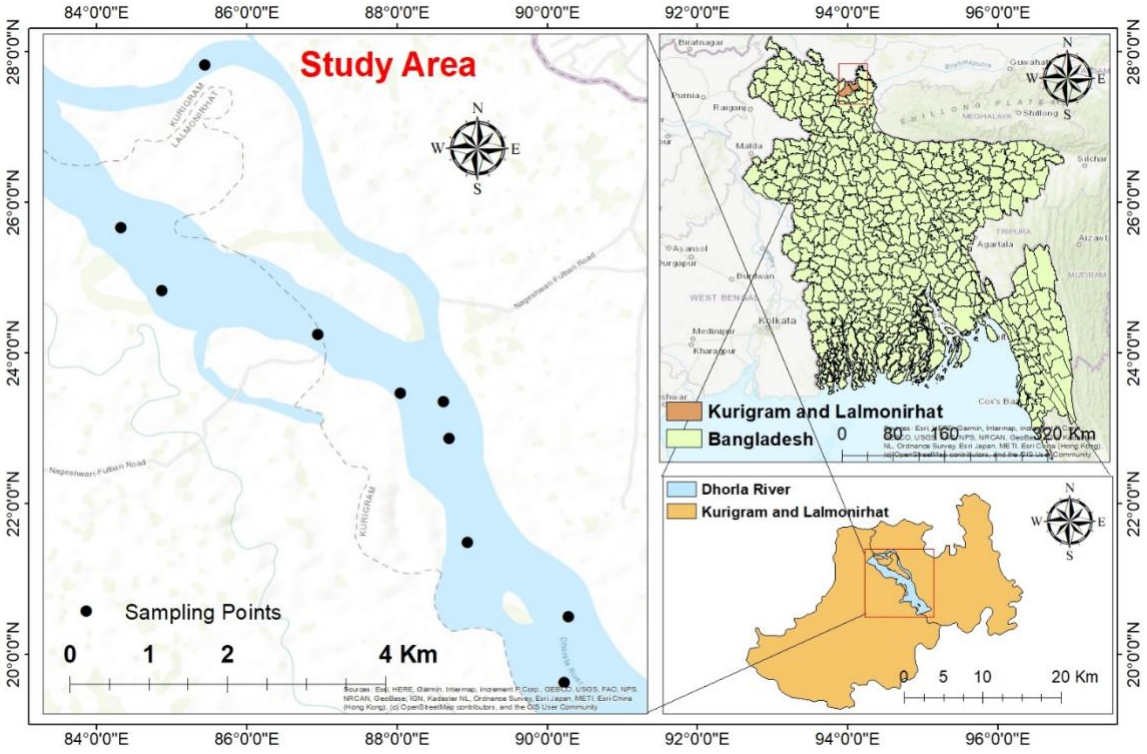


**Figure 3.2 Location of the study area showing specific location of sampling in the Dharla river of northern Bangladesh.**

## 3.3 Sample Collection Procedures

Using the required tools, sediment samples were methodically collected. A GPI pipe measuring 8 cm in diameter and 40 cm in height was used, and it was fitted with a sample remover and rubber stopper. The first step in the sample process was using a GPS device to determine the sampling position. The GPI pipe was then inserted, creating a hole that was 10 to 15 cm deep, and the upper aperture was sealed with a rubber cork. Three samples in total were taken from the same area, resulting in an equilateral triangle with a minimum of 100 metres between the sides. The sampling locations were placed thoughtfully at a distance of roughly one kilometre. Carefully unscrewing the pipe in a horizontal configuration allowed for its extraction. After the samples were gathered, they were labelled with their geographic coordinates and securely put in zip-locked bags.

**The sample collection information is presented in the following Table 3.1.**

| Sampling ID | Latitude | Longitude |
|---|---|---|
| D-1 | E 25.9638 | N 89.5002 |
| D-2 | E 25.9356 | N 89.5139 |
| D-3 | E 25.9347 | N 89.5197 |
| D-4 | E 25.9322 | N 89.5244 |
| D-5 | E 25.9278 | N 89.5253 |
| D-6 | E 25.9236 | N 89.5267 |
| D-7 | E 25.9181 | N 89.5208 |
| D-8 | E 25.9139 | N 89.5169 |
| D-9 | E 25.9056 | N 89.55 |
| D-10 | E 25.9006 | N 89.5361 |

To ensure complete moisture reduction, the gathered samples were first sun-dried to remove any remaining water, and then they were dried again at 85°C in an electric oven until they reached a consistent weight. To avoid contamination, all processes were carried out with the highest precision and protective hand gloves were worn. The dried samples were then sieved through a 0.25 mm mesh screen to remove any remaining organic contaminants. Every sample was ground using an agate mortar and pestle to produce a uniformly smooth grain size.

Following processing, the samples were meticulously placed inside polythene bags and sealed with an impulse sealer. Each sample included between 300 and 400 grams of silt. It is important to remember that a representative sample for a meteorite's chemical characterization usually weighs between 0.5 and 0.8 grams (Khan et al., 2015). Each sample in our investigation had a ground mass of approximately 300–400 grams, which was 400–800 times more than the ground mass of meteorite samples. Given the precise distance from the sluice gate, this implies that the samples we have taken are probably going to offer a representative geochemical history of the relevant stratum and the sampling point.

## 3.4 Steps of Sample Preparation

To achieve the results of HPGe and Instrumental Neutron Activation Analysis, a set of organised steps must be followed. These steps include sample preparation, collection, reactor irradiation, and analysis. Of these, sample preparation is the most important and requires careful attention to detail in order to get reliable results.

### *3.4.1 Drying*

In order to avoid any kind of contamination, the sediment samples are first dried in the sun with extreme caution. These sedimentary soils are then dried in a microwave oven with a temperature of 85°C until they reach a consistent weight. Petri dishes are carefully cleaned using ethanol and de-ionized water throughout this procedure, and they are subsequently dried in an oven. The specimens collected are placed within Petri dishes that have been labelled with an individual identification number that corresponds to the sample ID. The drying timeframes for each sample vary based on the moisture level of the sample.

**Figure 3.3 Sample drying in micro-oven**

### *3.4.2 Sieving*

The samples were sieved with a sieve having a 0.25 mm diameter of hole after the drying process was finished. The purpose of this sifting process was to remove any rocks, organic materials, or foreign items from the samples.

**Figure 3.4 Sieving of the soil sample**

### *3.4.3 Grinding*

In order to obtain a fine and consistent particle size in the samples, grinding is an important step in this procedure. Samples of sediment are pulverised with an agate pestle and mortar in order to achieve this. The main goal of the grinding process is to minimise the grain size in order to facilitate the packaging and weighing of the samples before they are exposed to radioactivity in the reactor. The agate pestle and mortar are properly cleaned with ethanol before each sample is ground.

**Figure 3.5 Grinding of the samples**

### *3.4.4 Weighing*

The sediments are enclosed by an impulse-sealed Teflon plastic square package with sides measuring about 2 cm before the samples are weighed. The sample package is covered by another square package made of the same material that is 2.5 cm on each side. First, a specific kind of paper is zeroed and placed on a digital electronic microbalance. The sample package is then put on the electronic digital microbalance, and the result is entered into a register. The sample is then placed on the paper within a digital electronic microbalance, then the register is also updated with

the reading. After that, the sample is placed into the sample packaging and sealed with an impulse sealer on the last side. Ultimately, the sample package is studied, and the results are entered into the register.

**Figure 3.6 Digital electronic microbalance and thermal sealer**

**Table 3.2 Weight of the sample and poly bag/pot(gm)**

| Sample ID | Weight of blank pot (gm) | Sample+ pot (gm) | Sample weight [g] | Density [g/ml] |
|---|---|---|---|---|
| D-1.1 | 10.57 | 139.38 | 128.81 | 0.89 |
| D-1.2 | 10.62 | 117.85 | 107.22 | 0.74 |
| D-1.3 | 10.06 | 162.50 | 152.45 | 1.05 |
| D-2.1 | 9.86 | 114.42 | 104.56 | 0.72 |
| D-2.2 | 10.61 | 122.63 | 112.02 | 0.77 |
| D-2.3 | 11.31 | 161.50 | 150.18 | 1.04 |
| D-3.1 | 10.42 | 110.90 | 100.48 | 0.69 |
| D-3.2 | 10.37 | 113.76 | 103.39 | 0.71 |
| D-3.3 | 10.82 | 159.38 | 148.56 | 1.02 |
| D-4.1 | 10.78 | 103.79 | 93.01 | 0.64 |
| D-4.2 | 11.26 | 145.98 | 134.72 | 0.93 |

| | | | | |
|---|---|---|---|---|
| D-4.3 | 10.70 | 108.08 | 97.38 | 0.67 |
| D-5.1 | 10.60 | 126.00 | 115.41 | 0.80 |
| D-5.2 | 10.62 | 105.27 | 94.65 | 0.65 |
| D-5.3 | 10.70 | 110.15 | 99.45 | 0.69 |
| D-6.1 | 9.43 | 112.66 | 103.24 | 0.71 |
| D-6.2 | 9.60 | 97.92 | 88.32 | 0.61 |
| D-6.3 | 10.51 | 131.86 | 121.34 | 0.84 |
| D-7.1 | 10.81 | 122.30 | 111.48 | 0.77 |
| D-7.2 | 10.95 | 139.24 | 128.29 | 0.88 |
| D-7.3 | 10.55 | 103.24 | 92.69 | 0.64 |
| D-8.1 | 11.01 | 89.63 | 78.62 | 0.54 |
| D-8.2 | 9.68 | 103.40 | 93.72 | 0.65 |
| D-8.3 | 10.77 | 104.30 | 93.54 | 0.65 |
| D-9.1 | 10.08 | 110.44 | 100.36 | 0.69 |
| D-9.2 | 10.04 | 129.95 | 119.92 | 0.83 |
| D-9.3 | 10.57 | 131.52 | 120.96 | 0.83 |
| D-10.1 | 10.92 | 115.51 | 104.59 | 0.72 |
| D-10.2 | 10.62 | 104.18 | 93.56 | 0.65 |
| D-10.3 | 10.68 | 89.69 | 79.01 | 0.54 |

## 3.5 Preparation of Sample for HPGe Detector

The typical setup for gamma-ray detection of radioactive materials consists of a computer-based multi-channel analyser, related electronics, and a semiconductor detector. High-purity or intrinsic germanium (HPGe) detectors are widely utilised because they can operate at very low temperatures by employing liquid nitrogen. These detectors are made up of a vacuum-sealed germanium crystal that is thermally connected to a copper rod, sometimes known as a "cold finger." High Purity Germanium (HPGe) detectors are semiconductor detectors that can detect gamma rays that are released during radioactive decay of a product nucleus. Gamma spectroscopic studies commonly

use HPGe detectors because of its higher resolution as compared to NI crystals. One way of measuring the amount of radiation that enters a building is through the free charge carriers produced by semiconductor detectors.

**Figure 3.7 Prepared samples**

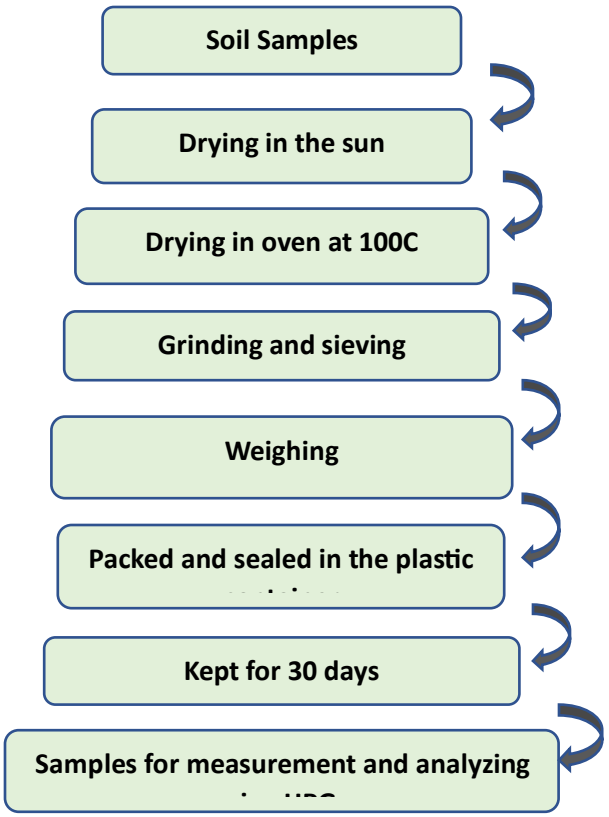


**Figure: 3.8 The flow chart of soil sample preparation**

## 3.6 Setup of the experiment

### *3.6.1 High Purity Germanium detector (HPGe)*

A computer-based multi-channel analyser, related electronics, and a semiconductor detector are the usual setup for detecting gamma rays from radioactive materials. In this configuration, hyper pure or intrinsic germanium (HPGe) detectors are frequently employed. Liquid nitrogen is used to operate these detectors at extremely low temperatures since the germanium crystal is vacuum-enclosed and thermally coupled to a copper rod, also known as a "cold finger." Semiconductor detectors can catch gamma rays released by the product nucleus, such as the High Purity Germanium (HPGe) type. Known for their higher resolution than Ni crystals, HPGe detectors are widely used in gamma spectroscopy investigations. Incoming radiation is detected and measured

using semiconductor detectors, which produce free charge carriers (Figure 3.12). The Atomic Energy Research Establishment (AERE) in Savar is home to the detector used in this study.

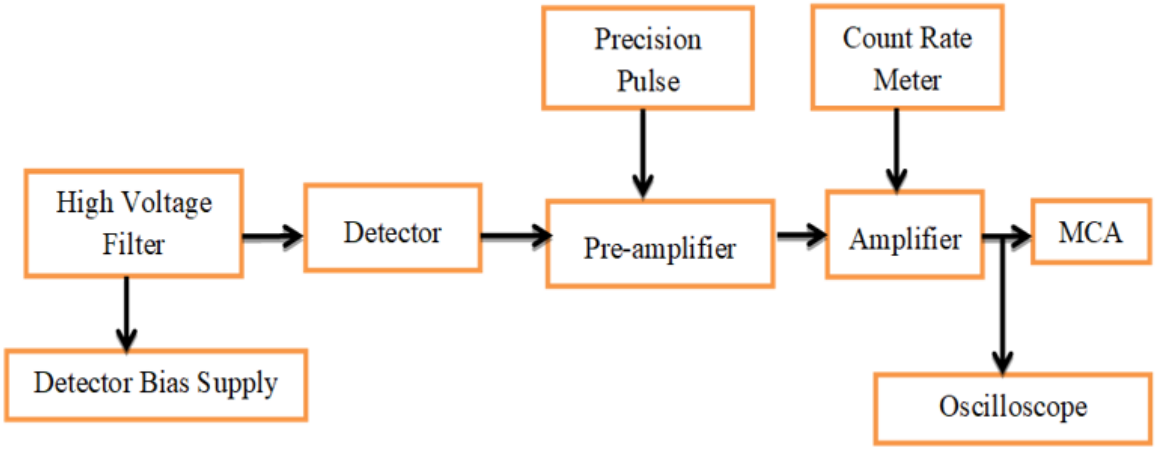


**Figure 3.9 Block diagram of gamma ray detector setup**

**Figure 3.10 HPGe detector system in BAEC, Savar, Dhaka**

### *3.6.2 Standard Gamma Ray sources*

For γ-spectrometer calibration, calibration sources are essential in labs that use gamma rays for scientific measurements. Calibration sources from Amershem International in the USA were used by the Institute of Nuclear Science & Technology (INST), AERE, Savar, Dhaka (Khan et al., 2021).

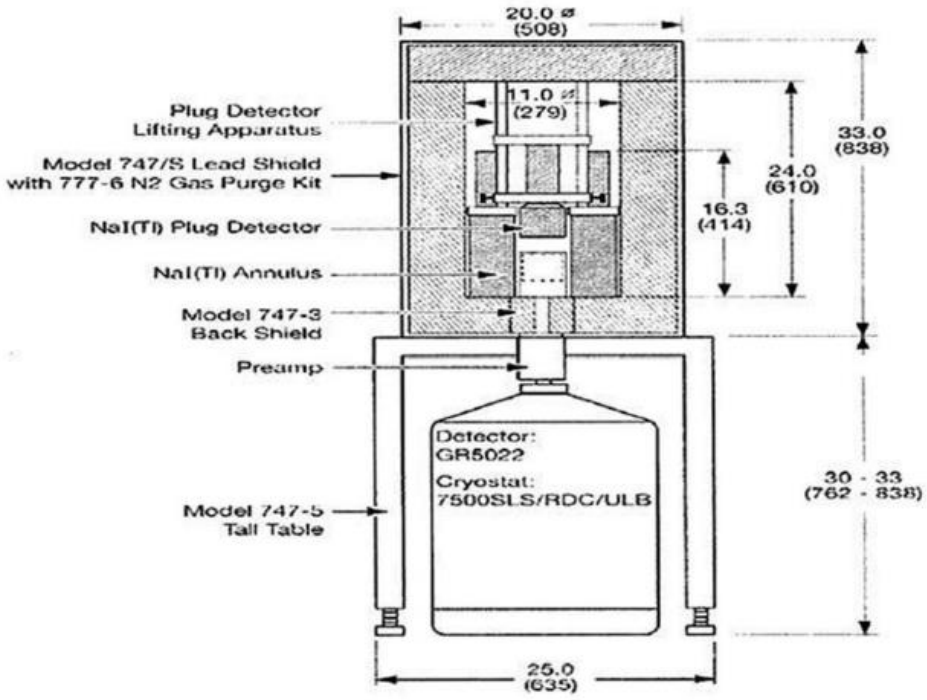


**Figure 3.11 Cross- sectional view of HPGe detector (Khan et al., 2021)**

### *3.6.3 Detector Parameters Calibration*

Spectra from the computerised Multichannel Analyzer (MCA) are necessary in gamma spectrometry to acquire information on peak position and count rate with respect to gamma energy. The gamma spectrometry system requires a gamma source with known energy in order to be

calibrated. In gamma spectrometry, peak locations are determined by the energy of gamma rays that are captured and found by the multichannel analyser (MCA). By comparing the number of channels to the detected gamma energy, calibration enables the identification of known radionuclides in an unknown sample. It is useless to concentrate on channel numbers unless measured energy is used to calibrate them. The number of channels or the height of the detector's output pulse can be used to measure the intensity of gamma rays.

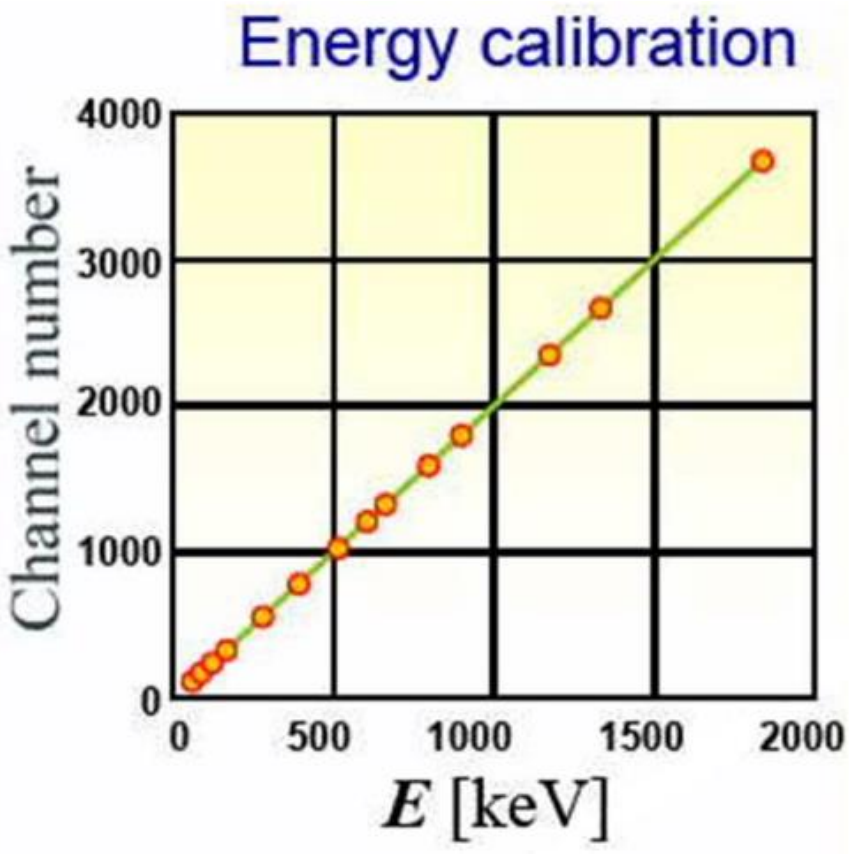


**Figure 3.12 The typical correlation between the channel number of gamma rays and their observed energies during energy calibration.**

### *3.6.4 HPGe Detector Efficiency Calibration*

Comprehending the detector's working principles in counting modes is essential to obtaining accurate radionuclide activity measurements. Matrix properties, source geometry, and the source-detector combination all affect the count rate. This can be problematic, particularly when there are a variety of matrices and geometries in the measurements (Usif et al., 2008). Therefore, evaluating the effectiveness of the current configuration is essential. Furthermore, to maximise γ-ray spectrometry, collection efficiencies at diverse energies is required to ascertain the activity of distinct radionuclides in the sample. The efficiency value at any given energy is obtained by the calibration of efficiency as a function of energy. According to Saegusa et al. (2004), accurate findings necessitate counting samples in the same conditions as those used for equipment calibration.

The HPGe detector's effectiveness in this investigation was assessed by contrasting it with references made from a solid matrix that had been calibrated using $^{226}$Ra standards. Standard sources were created with a collection of geometrically identical containers.

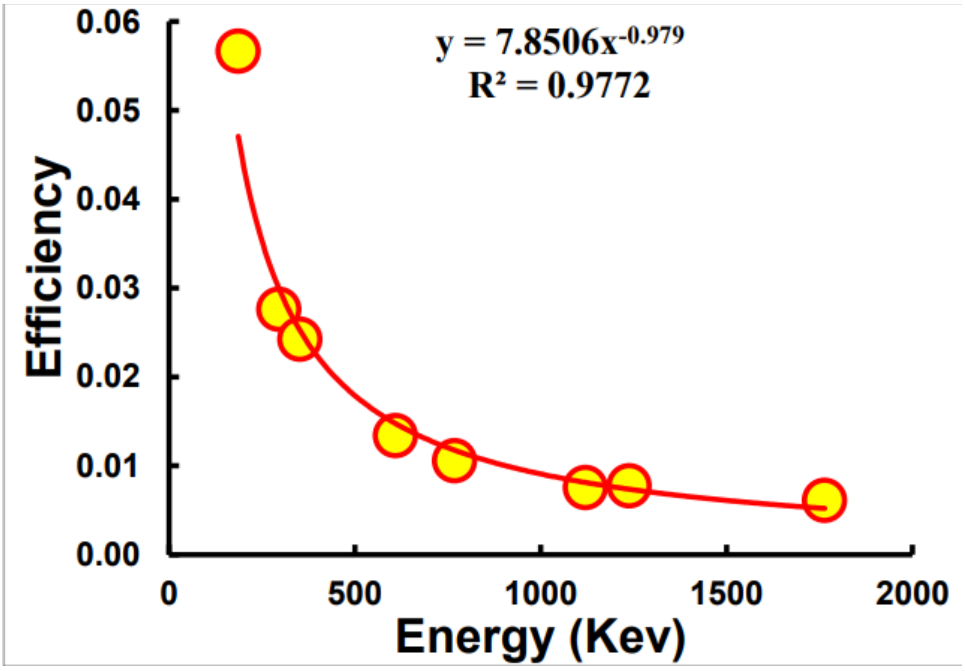


**Figure 3.13 Efficiency calibration curve of HPGe detector**

### *3.6.5 Lower Limit of Detection (LLD) of Radionuclides*

The lowest emission rate that a measurement device can detect is known as the lower limit of detection (LLD), sometimes known as the detection limit or least detectable emission rate (LDER). This limit is affected by a number of variables, including background, detector sensitivity, source-detector separation, sample geometry, radiation dose, and measurement length.

| Radionuclide | Energy in KeV | LLD (Bq) |
|---|---|---|
| $^{214}Pb$ | 295, 352 | 1.16 |
| $^{214}Bi$ | 609, 1238, 1378 | 1.06 |
| $^{228}Ac$ | 911, 969 | 1.10 |
| $^{208}Tl$ | 583,2614 | 0.90 |
| $^{40}K$ | 1460 | 25.91 |

**Table 3.3 Radionuclides' Lower Limit of Detection (Khan et al., 2021)**

### *3.6.6 Gamma Ray Detection*

In order to detect gamma rays, reference and test samples must first be exposed to radiation before being transferred to the HPGe detector. The gamma rays that the samples under study release are intended to be detected by the experimental apparatus.

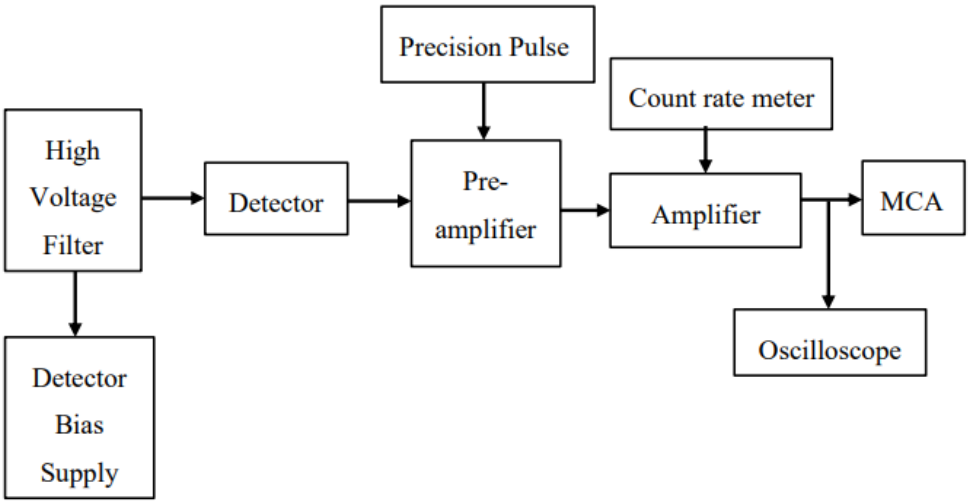


**Figure 3.14 Block Diagram of the gamma ray detection**

## 3.7 Preparation of sample for INAA

The sample container was placed inside the cover package—a separate package—after it had been weighed. After that, this cover package was marked with a special identification number that went with the sample ID it held. The cover package and sample container were almost the same size and shape. These packages were then suitably stored in anticipation of being exposed to neutron radiation. For the purposes of the tests, each sample container included around 50 mg of dried crushed silt.

Three reference materials were used in this investigation for the aim of relative standardisation: IAEA-Soil-7, IAEA-SL-1, and one standardised reference material, INST-1633b. The preparation of each of these criteria was done in the same way as the samples. For irradiation, the standards and samples were both put in a vial. Three foils, three standards, and the samples were all inside the vial. IAEA-Soil-7 and IAEA-SL-1 were the control samples, and INST-1633b was used as the reference.

## 3.8 Experimental setup for INAA

### *3.8.1 Application of INAA*

When compared to other techniques like atomic absorption spectroscopy (AAS), inductively coupled plasma spectroscopy (ICPS), and total reflection X-ray fluorescence spectroscopy (TR-XRE) under different conditions, INAA is a very successful approach for elemental analysis. Thus, it is essential to retain neutrality when assessing INAA's activity. A few of the more notable analytical traits of INAA are listed below:

- Shows a notable level of resilience against interference and matrix effects.
- Rarely runs into blank areas when analysing.
- Demonstrates adaptability and sensitivity in identifying trace and small components in a variety of matrices.
- Has a greater chance of being accurate than other analytical techniques since it is supported by a theoretical framework that is well-understood and permits a thorough evaluation of uncertainty.
- Unlike most other analytical techniques that rely on electronic principles, it is entirely autonomous as a nuclear-based technique.
- Possesses the capacity for non-destructive examination.
- The unique characteristics of induced radionuclides guarantee high specificity.
- Permits multi-element determination, frequently enabling the examination of 30–40 components in different matrices.

### *3.8.2 Irradiation*

The Bangladesh Atomic Energy Commission's 3 MW TRIGA Mark-II research reactor in Savar underwent two irradiation processes. In the first approach, all the samples and standards were subjected to a thermo neutron flux of 2.11×10^13 neutrons every square centimetre per second

over 7 minutes with a power level of 2.4 MW. This was done over an extended period of time. In the second procedure, each sample was individually exposed to a short irradiation for one minute at an intensity of 250 kW, or 5.28×10^12 neutrons every square centimetre per second.

In addition, three monitor foils composed of IRMM-530RA Al-0.1% Au (0.1 mm foil) was additionally exposed to radiation in order to ascertain the neutron flux gradient inside the sample stack in the lengthy irradiation scheme. These foils were positioned in the sample stack at the top, middle, and bottom. The samples got extremely radioactive after the lengthy irradiation, so as a precaution, they weren't handled right away. Rather, they spent two days in a protected area. Usually, this irradiation equipment is called the G-ring.

**Table 3.4 Short Irradiation Criteria of 3 MW TRIGA MARK-II reactor**

| Research reactor | 3 MW TRIGA MARK-II |
|---|---|
| Neutron flux | ~5.28 ×1012 $cm^{-2}s^{-1}$ |
| Reactor power | 250kW |
| Irradiation time | 60 second |
| Irradiation facility | G-ring |

**Table 3.5 Long Irradiation Criteria of 3 MW TRIGA MARK-II reactor**

| **Research reactor** | **3 MW TRIGA MARK-II** |
|---|---|
| Neutron flux | ~2.11×1013 $cm^{-2}s^{-1}$ |
| Reactor power | 500 kW |
| Irradiation time | 1 hour |
| Irradiation facility | G-ring |

**Figure 3.15 Sending and receiving centre for sample vial in BAEC, Savar**

### *3.8.3 Gamma Ray Counting*

After the radiation, a digital gamma spectrometer (ORTEC, DSPEC JrTM) and a high purity germanium (HPGe) detector with particular properties (CANBERRA, 25% relative efficiency, 1.8 keV resolution at 1332.5 keV of 60Co) were used to perform gamma-ray observations.

For samples that were exposed to brief radiation, two counting rounds were conducted. After around 300 seconds for decay time, the first counting happened, and after two to three hours of decay time, or 600 seconds, the second counting happened. Samples that were exposed to extensive radiation underwent a longer counting procedure. Following a decay period of two to three days, the initial counting session began and lasted for 3600 seconds. Following a decay period of 7–10 days, the following counting session lasted 7200 seconds, whereas the third counting session followed a decay period of 2-3 weeks, spanning 8–12 hours. With this method, short- and long-lived radionuclides may be distinguished from short- and long-term radiation.

All irradiated samples and approved reference materials underwent gamma spectrometry analysis utilising a PC-based HPGe detector linked to a digital gamma spectrometry equipment. As shown

in Figures 4.10 and 4.11 (Wyttenbach, 1971), data collecting was managed using the Genie-2000 software from Canberra and MAESTRO-32 from ORTEC. The Hypermet PC version 5.12 software was used to do the gamma peak analysis.

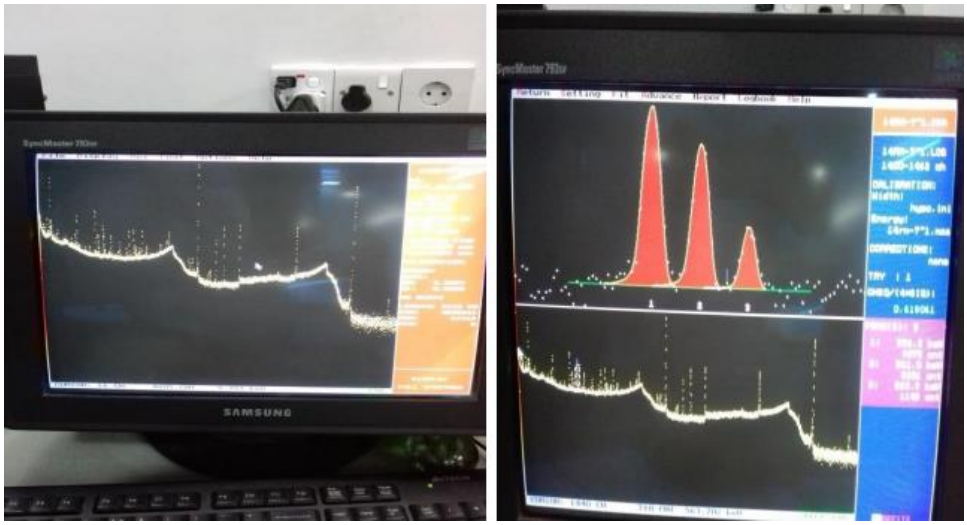

**Figure 3.16 Gamma peak analysis with Hypermet PC (5.12)**

### *3.8.4 Concentration Calculation*

The relative standardization method was used to calculate concentrations, and the given equations were used in the process. To ascertain the concentrations of various components, these findings were entered into an Excel spreadsheet. For this, the relative INAA-specific activation equation was applied.

$$\frac{\text{Weight of element "x" in sample}}{\text{Weight of element "x" in standard}} = \frac{A_{x^*} in\ sample \times (e^{\lambda t})_{sam}}{A_{x^*} in\ sample \times (e^{\lambda t})_{std}}$$

The weight of element "x" in the sample can be calculated by taking into account the activities of x* in both the sample and the standard, as well as the decay times of the sample and standard and the weight of "x" in the standard.

### *3.8.5 Accuracy and Precisions*

Accuracy and precision are crucial concepts in elemental analysis, and they are both carefully computed in each analysis. Even the smallest oversight can result in major problems and imprecisions and inaccuracies in the data. As a measure of statistical variability, precision is defined here as a representation of random errors. Furthermore, accuracy is defined as a systematic error representation, denoting a statistical bias. The degree to which measurements of a quantity agree with its true value is referred to as the measuring system's accuracy in science, engineering, and statistics. Regarding reproducibility and repeatability, a measuring system's accuracy indicates how well repeated measurements conducted in the same way provide consistent outcomes.

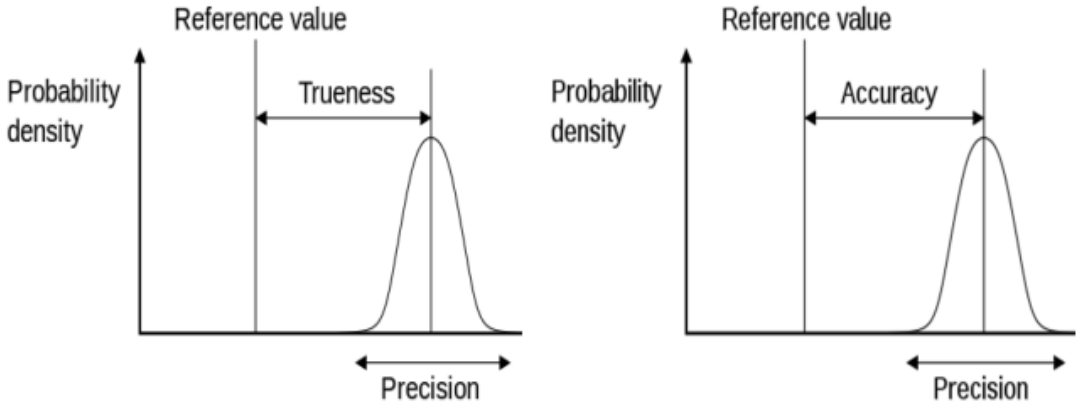


**Figure 3.17 Graphical presentation of accuracy and precision**

## 3.9 Secondary data sources

A range of scientific journals, technical reports, books, review articles, and research papers were used to collect secondary data and information. Then, using this chosen secondary data, other metadata was created, including multiple standard values for calculating different indices. Furthermore, the secondary data and information obtained were employed to compare the results and conclusions of the current investigation with previously collected data and information. This made it easier to comprehend and assess the condition of the research topic today as well as the caliber and outcomes of the investigation.

# Chapter 04

# Data Analysis

### 4.1 Various Radiological and Environmental Indicators

The mathematical formulas used for various radiological indices; Radium equivalent activity ($Ra_{eq}$), External hazard index ($H_{ex}$), Internal hazard index ($H_{in}$), Absorbed dose rate (D), Annual effective dose rate ($E_{aed}$), Gamma representative level index ($I_{\gamma}$), Activity utilization index (AUI) and Excess lifetime cancer risk (ELCR) are:

***4.1.1 $Ra_{eq}$ or Radium equivalent activity*** - Naturally Occurring Radioactive Materials (NORM) concentrations in environmental components like sediments, soil, or dust often exhibit variations. To address this variability and assess potential radiation risks associated with γ-radiation, the $Ra_{eq}$ index has been commonly utilized (Shuaibu et al., 2017; Ravisankar et al., 2015). The calculation method is outlined below.

$$Ra_{eq} = \frac{A_{Ra}}{370} + \frac{A_{Th}}{259} + \frac{A_K}{4810} \times 370$$

(1)

According to Isinkaye and Emelue (2015), the activity concentrations of $^{226}Ra$, $^{232}Th$, and $^{40}K$ (expressed in $Bq.kg^{-1}$) are represented as $A_{Ra}$, $A_{Th}$, and $A_K$, respectively.

***4.1.2 External hazard index ($H_{ex}$) and Internal hazard index ($H_{in}$)*** - Beretka and Mathew developed the external hazard ($H_{ex}$) index, which is an additional radiation hazard index used to evaluate the rate of indoor radiation exposure from external exposure to gamma radiation emitted by naturally occurring radionuclides found in residential building materials (J. Beretka & P. J. Mathew, 1985). Analyse the rate at which gamma radiation from naturally occurring radionuclides present in residential building materials is exposed internally (Mbonu & Ben, 2021).

$$H_{ex} = \frac{A_{Ra}}{370\ BqKg^{-1}} + \frac{A_{Th}}{259\ BqKg^{-1}} + \frac{A_K}{4810\ BqKg^{-1}}$$

(2)

$$H_{in} = \frac{A_{Ra}}{185\ BqKg^{-1}} + \frac{A_{Th}}{259\ BqKg^{-1}} + \frac{A_K}{4810\ BqKg^{-1}}$$

(3)

***4.1.3 Absorbed dose rate (D)*** - The amount of energy that is ionising radiation transfers to matter per unit mass is measured by a metric called absorption dose (Windsor & Michaels, 2007). The approach described by Isinkaye and Emelue (2015) and Ravisankar et al. (2015) can be used to

approximate the associated radiation dose rate given the correlation between the specific effects of terrestrial γ-radiation and Naturally Occurring Radioactive Materials (NORMs).

$$D\ (nGyh^{-1}) = 0.462\ A_{Ra} + 0.604\ A_{Th} + 0.0417\ A_{g} \quad (4)$$

The UNSCEAR (2000) specification states that the conversion coefficients for converting the radioactive concentrations of $^{226}$Ra, $^{232}$Th, and $^{40}$K into dose rates (in nGy/h per Bq/kg) are 0.462, 0.604, and 0.0417, respectively.

***4.1.4 $E_{aed}$ or Annual effective dose rate*** - Within the framework for radioactive protection developed by the International Commission on radioactive Protection (ICRP), effective dose is one of the dosage metrics. It allows the aggregation of organ doses from various amounts and types of radiation, both internal and external, to calculate an all-inclusive effective dose. It does this by taking into account the type of radiation and the properties of each organ or tissue absorbing radiation (Boumala et al., 2019).

Valued by (Eq. 5) under UNSCEAR (2000) to compute $E_{aed}$, D ($nGyh^{-1}$) is used.

$$E_{aed} = D(nGyh-1) \times 8760(hy^{-1}) \times 0.2 \times 0.7 \times 10^{-6} \quad (5)$$

***4.1.5 Gamma representative level index (Iγ)*** - The European Commission's radiation hazard index, or $I_\gamma$, can be used to estimate the risk of gamma radiation, especially when dealing with naturally occurring radionuclides (Bavarnegin et al., 2013).

$$I_\gamma = \frac{A_{Ra}}{150} + \frac{A_{Th}}{100} + \frac{A_K}{1500} \quad (6)$$

***4.1.6 Activity utilization index (AUI)*** - It is utilized to estimate the sum of radionuclides in soil (Joel et al., 2019).

$$AUI = \frac{A_{Ra}}{50BqKg^{-1}} \times f_{Ra} + \frac{A_{Th}}{50BqKg^{-1}} \times f_{Th} + \frac{A_K}{50BqKg^{-1}} \times f_K \quad (7)$$

The activity concentration of $^{226}$Ra, $^{232}$Th, and $^{40}$K (Bq. $Kg^{-1}$) are expressed here by $A_{Ra}$, $A_{Th}$, and $A_K$, respectively; $f_{Ra}$(=0.462), $f_{Th}$(=0.604) and $f_K$ (=0.041) (Khan et al., 2021).

***4.1.7 Excess lifetime cancer risk (ELCR)*** - Determines the potential of any element to cause cancer (Qureshi et al., 2014). It can be calculated by (Eq. 8) (Kolo et al., 2015).

$$ELCR = E_{aed} \times A_{lf} \times R_f \quad (8)$$

$A_{lf}$ is the average lifespan (70 years) and $R_f$ is the cancer risk factor. (ICRP, 1990: $0.5x10^{-4}$ $Sv^{-1}$) for public exposure (Abedin & Khan, 2022).

## 4.2 Statistical analysis

The analytical data sets of the radionuclides were organized in an excel sheet and their graphical illustrations were formed for understanding the relationships of natural radionuclides, their Radium equivalent activity ($Ra_{eq}$), External hazard index ($H_{ex}$), Internal hazard index ($H_{in}$), Absorbed dose rate (D), Annual effective dose rate ($E_{aed}$), Gamma representative level index ($I_\gamma$), Activity utilization index (AUI) and Excess lifetime cancer risk (ELCR).

# Chapter 05

# Result and Discussion

### 5.1 Statistical analysis result of occurrence and NORMs distribution

The radioactive amounts of naturally occurring radioactive materials (NORMs), namely $^{226}Ra$, $^{232}Th$, and $^{40}K$, were evaluated in this study. Thirty sediment samples in all were taken from ten distinct sites in the Dharla River Basin (DRB). HPGe gamma spectrometry was used to determine NORMs, and the results, together with statistical analysis and other information from the related literature, are shown in Table 5.1. The NORM profile comprises the following parameters: lowest and maximum values, relative standard deviation (RSD), standard deviation (±SD), mean abundance (n=30), and associated analytical uncertainties (%). Table 5.1 (Rudnick and Gao, 2014) also includes the upper continental crust (UCC) values and comparative data from domestic and international sources.

**Table 5.1 A comparison of activity concentrations of 226Ra, 232Th and 40K radionuclides (in Bqkg-1) and the radiological indices associated from this study with the literature data on Dharla River**

| | $^{226}Ra$ | | $^{232}Th$ | | $^{40}K$ | |
|---|---|---|---|---|---|---|
| | **[Bqkg$^{-1}$]** | ± | **[Bqkg$^{-1}$]** | ± | **[Bqkg$^{-1}$]** | ± |
| **D-1.1** | 55.4 | 4.2 | 44.3 | 3.3 | 567 | 66 |
| **D-1.2** | 90.9 | 9.9 | 71.9 | 3.0 | 820 | 81 |
| **D-1.3** | 68.3 | 3.8 | 45.4 | 2.2 | 443 | 46 |
| **D-2.1** | 38.8 | 3.8 | 31.9 | 3.5 | 560 | 69 |
| **D-2.2** | 51.2 | 6.6 | 86.6 | 3.2 | 651 | 73 |
| **D-2.3** | 47.3 | 4.5 | 50.8 | 2.9 | 485 | 69 |
| **D-3.1** | 59.2 | 5.3 | 40.9 | 3.3 | 496 | 55 |
| **D-3.2** | 79.7 | 5.6 | 43.1 | 3.2 | 716 | 76 |
| **D-3.3** | 36.6 | 3.5 | 21.8 | 2.5 | 481 | 53 |
| **D-4.1** | 67.2 | 5.6 | 38.6 | 3.4 | 915 | 90 |
| **D-4.2** | 30.6 | 3.3 | 16.9 | 2.2 | 540 | 50 |
| **D-4.3** | 72.8 | 5.1 | 34.5 | 3.2 | 841 | 85 |

| | | | | | | |
|---|---|---|---|---|---|---|
| **D-5.1** | 33.5 | 4.9 | 25.4 | 3.0 | 512 | 70 |
| **D-5.2** | 60.7 | 6.0 | 33.4 | 3.3 | 667 | 86 |
| **D-5.3** | 49.2 | 5.8 | 29.8 | 3.2 | 544 | 56 |
| **D-6.1** | 71.9 | 5.7 | 46.4 | 3.2 | 833 | 78 |
| **D-6.2** | 36.1 | 4.8 | 27.1 | 3.5 | 693 | 82 |
| **D-6.3** | 69.5 | 5.1 | 43.9 | 2.7 | 705 | 63 |
| **D-7.1** | 63.7 | 4.2 | 27.1 | 3.1 | 498 | 69 |
| **D-7.2** | 75.2 | 4.9 | 50.6 | 2.8 | 739 | 63 |
| **D-7.3** | 121.2 | 5.7 | 81.4 | 3.8 | 763 | 88 |
| **D-8.1** | 56.7 | 7.1 | 33.0 | 4.3 | 1008 | 101 |
| **D-8.2** | 71.3 | 3.2 | 54.9 | 3.8 | 750 | 75 |
| **D-8.3** | 52.9 | 5.5 | 29.1 | 3.3 | 844 | 92 |
| **D-9.1** | 34.3 | 3.8 | 22.9 | 2.9 | 682 | 57 |
| **D-9.2** | 30.4 | 2.1 | 15.1 | 0.7 | 225 | 14 |
| **D-9.3** | 47.1 | 4.7 | 23.5 | 2.9 | 648 | 58 |
| **D-10.1** | 70.1 | 6.8 | 34.8 | 3.3 | 733 | 82 |
| **D-10.2** | 84.0 | 7.2 | 56.5 | 2.9 | 768 | 84 |
| **D-10.3** | 94.9 | 6.8 | 53.6 | 4.9 | 763 | 91 |
| **Mean (n=30)** | 60.7 | | 40.5 | | 663 | |
| **SD (1σ)** | 21.3 | | 17.6 | | 165 | |
| **RSD (%)** | 35.1 | | 43.4 | | 24.9 | |
| **Min.** | 30.4 | | 15.1 | | 225 | |
| **Max.** | 121.2 | | 86.6 | | 1008 | |
| | | | | | | |
| **Literature work** | | | | | | |
| **Recommended values[a]** | 35 | | 30 | | 400 | |

| | | | | | | |
|---|---|---|---|---|---|---|
| **Milos Island, Greece[o]** | 70.0 | | 75.0 | | 890 | |
| **Langkawi Island, Malaysia[p]** | 1478 | | 718 | | 103 | |
| **Atticocycladic beach, Greece[q]** | 142 | | 525 | | 732 | |
| **Orissa sea beach, India[r]** | 220 | | 2500 | | 120 | |
| **Niger River, Nigeria[k]** | 75.3 | | 9.64 | | 231 | |
| **Lake Van Basin, Turkey[l]** | 50.0 | | 60.2 | | 1010 | |
| **Tagus river, Spain[m]** | 42.0 | | 63.0 | | 572 | |
| **Danube, Serbia[n]** | 32.0 | | 36.0 | | 445 | |
| **Karnaphuli river, Bangladesh[b]** | 35.9 | | 65.5 | | 272 | |
| **Shango river, Bangladesh[b]** | 27.8 | | 57.5 | | 255 | |
| **Teesta river, Bangladesh[c]** | 67.8 | | 104.2 | | 983 | |

| | | | | | | |
|---|---|---|---|---|---|---|
| **Wei River, China[d]** | 21.8 | | 33.1 | | 833 | |
| **Ponnaiyar river, India[e]** | 7.31 | | 46.9 | | 384 | |
| **Vaigai River, India[f]** | 7.45 | | 33.8 | | 448 | |
| **Palaru river, India[g]** | 9.35 | | 49.6 | | 704 | |
| **HGI Rivers, Pakistan[h]** | 50.7 | | 70.2 | | 532 | |
| **Nile river, Egypt[i]** | 16.3 | | 12.9 | | 200 | |
| **Oguta Lake, Nigeria[j]** | 47.9 | | 55.4 | | 1023 | |
| **Cox's Bazar (raw sand), Bangladesh[s]** | 2450 | | 3800 | | 170 | |

Table 5.1 Continued

| | **Radium equivalent activity ($Ra_{eq}$)** | **External hazard index ($H_{ex}$)** | **Internal hazard index ($H_{in}$)** | **Absorbed dose rate (D)** | **Annual effective dose rate ($E_{aed}$)** | **Gamma representative level index ($I_{\gamma}$)** | **Activity utilization index (AUI)** | **Excess lifetime cancer risk (ELCR)** |
|---|---|---|---|---|---|---|---|---|
| | [$Bqkg^{-1}$] | | | [$\eta Gyh^{-1}$] | [$mSvy^{-1}$] | | | |

| | | | | | | | | |
|---|---|---|---|---|---|---|---|---|
| **D-1.1** | 162 | 0.44 | 0.59 | 76.8 | 0.094 | 1.19 | 1.09 | 3.30x10^04 |
| **D-1.2** | 257 | 0.69 | 0.94 | 120.8 | 0.148 | 1.87 | 1.77 | 5.19x10^04 |
| **D-1.3** | 167 | 0.45 | 0.64 | 78.3 | 0.096 | 1.21 | 1.22 | 3.36x10^04 |
| **D-2.1** | 128 | 0.34 | 0.45 | 61.1 | 0.075 | 0.95 | 0.79 | 2.62X10^04 |
| **D-2.2** | 225 | 0.61 | 0.75 | 104.6 | 0.128 | 1.64 | 1.57 | 4.49X10^04 |
| **D-2.3** | 157 | 0.43 | 0.55 | 73.7 | 0.090 | 1.15 | 1.09 | 3.16X10^04 |
| **D-3.1** | 156 | 0.42 | 0.58 | 73.5 | 0.090 | 1.13 | 1.08 | 3.15X10^04 |
| **D-3.2** | 196 | 0.53 | 0.75 | 93.4 | 0.115 | 1.44 | 1.32 | 4.01X10^04 |
| **D-3.3** | 105 | 0.28 | 0.38 | 50.5 | 0.062 | 0.78 | 0.64 | 2.17X10^04 |
| **D-4.1** | 193 | 0.52 | 0.70 | 93.2 | 0.114 | 1.44 | 1.16 | 4.00X10^04 |
| **D-4.2** | 96 | 0.26 | 0.34 | 47.2 | 0.058 | 0.73 | 0.53 | 2.03X10^04 |
| **D-4.3** | 187 | 0.50 | 0.70 | 90.1 | 0.110 | 1.39 | 1.16 | 3.87X10^04 |
| **D-5.1** | 109 | 0.30 | 0.39 | 52.6 | 0.065 | 0.82 | 0.66 | 2.26X10^04 |
| **D-5.2** | 160 | 0.43 | 0.60 | 76.6 | 0.094 | 1.18 | 1.02 | 3.29X10^04 |
| **D-5.3** | 134 | 0.36 | 0.49 | 63.9 | 0.078 | 0.99 | 0.86 | 2.74X10^04 |
| **D-6.1** | 202 | 0.55 | 0.74 | 96.8 | 0.119 | 1.50 | 1.29 | 4.15X10^04 |
| **D-6.2** | 128 | 0.35 | 0.44 | 62.4 | 0.077 | 0.97 | 0.72 | 2.68X10^04 |
| **D-6.3** | 186 | 0.50 | 0.69 | 88.7 | 0.109 | 1.37 | 1.23 | 3.81X10^04 |
| **D-7.1** | 141 | 0.38 | 0.55 | 67.0 | 0.082 | 1.03 | 0.96 | 2.88X10^04 |
| **D-7.2** | 204 | 0.55 | 0.76 | 97.0 | 0.119 | 1.50 | 1.37 | 4.16X10^04 |
| **D-7.3** | 296 | 0.80 | 1.13 | 138.4 | 0.170 | 2.13 | 2.17 | 5.94X10^04 |
| **D-8.1** | 181 | 0.49 | 0.64 | 88.7 | 0.109 | 1.38 | 1.00 | 3.81X10^04 |
| **D-8.2** | 208 | 0.56 | 0.75 | 98.3 | 0.121 | 1.52 | 1.38 | 4.22X10^04 |
| **D-8.3** | 159 | 0.43 | 0.57 | 77.7 | 0.095 | 1.21 | 0.91 | 3.33X10^04 |
| **D-9.1** | 120 | 0.32 | 0.42 | 58.5 | 0.072 | 0.91 | 0.65 | 2.51X10^04 |
| **D-9.2** | 69 | 0.19 | 0.27 | 32.8 | 0.040 | 0.50 | 0.48 | 1.41X10^04 |
| **D-9.3** | 131 | 0.35 | 0.48 | 63.4 | 0.078 | 0.98 | 0.77 | 2.72X10^04 |
| **D-10.1** | 176 | 0.48 | 0.67 | 84.5 | 0.104 | 1.30 | 1.13 | 3.63X10^04 |
| **D-10.2** | 224 | 0.60 | 0.83 | 105.9 | 0.130 | 1.64 | 1.52 | 4.55X10^04 |
| **D-10.3** | 230 | 0.62 | 0.88 | 108.9 | 0.134 | 1.68 | 1.59 | 4.68X10^04 |

| | | | | | | | | |
|---|---|---|---|---|---|---|---|---|
| **Mean (n=30)** | 170 | 0.46 | 0.62 | 80.8 | 0.099 | 1.25 | 1.10 | 3.47X10^04 |
| **SD (1σ)** | 59 | 0.16 | 0.22 | 27.6 | 0.034 | 0.43 | 0.42 | 1.19X10^04 |
| **RSD (%)** | 99 | 0.27 | 0.36 | 44.2 | 0.054 | 0.68 | 0.85 | 1.90X10^04 |
| **Min.** | 59 | 0.16 | 0.22 | 27.6 | 0.034 | 0.50 | 0.48 | 1.41X10^04 |
| **Max.** | 296 | 0.80 | 1.13 | 138.4 | 0.170 | 2.13 | 2.17 | 5.94X10^04 |
| | | | | | | | | |
| **Literature work** | | | | | | | | |
| **Recommended values[a]** | **370** | **<1** | **<1** | **55** | **0.46** | **1.00** | 2.00 | **$2.90\times10^{-4}$** |
| **Milos Island, Greece[o]** | 246 | 0.66 | 0.85 | 116.0 | 0.14 | 1.81 | 1.63 | 4.98X10^04 |
| **Langkawi Island, Malaysia[p]** | 2513 | 6.79 | 10.78 | 1133.0 | 1.39 | 17.10 | 22.34 | 4.86X10^04 |
| **Atticocycladic beach, Greece[q]** | 949 | 2.56 | 2.95 | 422.0 | 0.52 | 6.68 | 7.71 | 1.81X10^04 |
| **Orissa sea** | 3804 | 10.27 | 10.87 | 1659.1 | 2.03 | 26.55 | 32.24 | 7.12X10^04 |

| | | | | | | | | |
|---|---|---|---|---|---|---|---|---|
| **beach, India[r]** | | | | | | | | |
| **Niger River, Nigeria[k]** | 107 | 0.29 | 0.49 | 50.4 | 0.06 | 0.75 | 0.83 | 2.16X10^04 |
| **Lake Van Basin, Turkey[l]** | 214 | 0.58 | 0.71 | 102.6 | 0.13 | 1.61 | 1.27 | 4.40X10^04 |
| **Tagus river, Spain[m]** | 176 | 0.48 | 0.59 | 82.4 | 0.10 | 1.29 | 1.20 | 3.54X10^04 |
| **Danube, Serbia[n]** | 118 | 0.32 | 0.40 | 55.7 | 0.07 | 0.87 | 0.77 | 2.39X10^04 |
| **Karnaphuli river, Bangladesh[b]** | 151 | 0.41 | 0.50 | 68.6 | 0.08 | 1.08 | 1.15 | 2.94X10^04 |
| **Shango river, Bangladesh[b]** | 130 | 0.35 | 0.43 | 59.2 | 0.07 | 0.93 | 0.97 | 2.54X10^04 |
| **Teesta river, Bangladesh[c]** | 292 | 0.79 | 0.97 | 137.0 | 0.17 | 2.15 | 1.97 | 5.88X10^04 |

| | | | | | | | | |
|---|---|---|---|---|---|---|---|---|
| **Wei River, China[d]** | 133 | 0.36 | 0.42 | 65.4 | 0.08 | 1.03 | 0.67 | 2.81X10^04 |
| **Ponnaiyar river, India[e]** | 104 | 0.28 | 0.30 | 48.5 | 0.06 | 0.77 | 0.66 | 2.08X10^04 |
| **Vaigai River, India[f]** | 90.3 | 0.24 | 0.26 | 43.1 | 0.05 | 0.69 | 0.51 | 1.85X10^04 |
| **Palaru river, India[g]** | 134 | 0.36 | 0.39 | 64.4 | 0.08 | 1.03 | 0.74 | 2.77X10^04 |
| **HGI Rivers, Pakistan[h]** | 192 | 0.52 | 0.66 | 89.1 | 0.11 | 1.39 | 1.36 | 3.83X10^04 |
| **Nile river, Egypt[i]** | 50.2 | 0.14 | 0.18 | 23.9 | 0.03 | 0.37 | 0.32 | 1.03X10^04 |
| **Oguta Lake, Nigeria[j]** | 206 | 0.56 | 0.69 | 99.2 | 0.12 | 1.55 | 1.20 | 4.26X10^04 |
| **Cox's Bazar (raw sand), Bangladesh[s]** | 7897 | 21.33 | 27.95 | 3498.8 | 4.29 | 54.45 | 68.56 | 1.50X10^02 |

Adjusting for process blank corrections and counting statistics are the sources of errors at the individual level; Radium equivalent activity ($Ra_{eq}$)($BqKg^{-1}$), External hazard index ($H_{ex}$), Internal hazard index ($H_{in}$), Absorbed dose rate (D) [$\eta Gyh^{-1}$], Annual effective dose rate ($E_{aed}$) [$mSvy^{-1}$], Gamma representative level index ($I_{\gamma}$), Activity utilization index (AUI) and Excess lifetime cancer risk (ELCR).

Florou, H., Kritidis, P., (1991). Khandaker, M. U., Asaduzzaman, K., Sulaiman, A. F. B., Bradley, D. A., & Isinkaye, M. O., (2018). Papadopoulos, A., Koroneos, A., Christofides, G., Papadopoulou, L., Tzifas, I., & Stoulos, S., (2016). Mohanty, A. K., Sengupta, D., Das, S. K., Saha, S. K., & Van, K. V., (2004). Faweya, E. B., Oniya, E. O., & Ojo, F. O., (2013). Zorer, Ö. S., (2019). Ibrahiem, N.M., Abd El Ghani, A.H., Shawky, S.M., Ashraf, E.M., Farouk, M.A., (1993). Krmar, M., Slivka, J., Varga, E., Bikit, I., Vesković, M., (2009). Chowdhury, M.I., Alam, M.N., Hazari, S.K.S., (1999). Khan, R., Islam, H.M. T., Islam, A.R.M.T., (2021). Lu, X., Zhang, X., & Wang, F., (2007). Suresh, G., Ramasamy, V., Meenakshisundaram, V., Venkatachalapathy, R., Ponnusamy, V., (2011). Ramasamy, V., Paramasivam, K., Suresh, G., Jose, M.T., (2014). Ramasamy, V., Suresh, G., Rajkumar, P., Murugesan, S., Mullainathan, S., & Meenakshisundaram, V., (2011). Qureshi, A.A., Tariq, S., Ud-Din, K., Manzoor, S., Calligaris, C., Waheed, A., (2014). EI-Gamal, A., Nasr, S., EI-Taher, A., 2007. Isinkaye, M.O., Emelue, H. U., (2015). Sasaki, T., Rajib, M., Akiyoshi, M., Kobayashi, T., Takagi, I., Fujii, T., & Zaman, M. M., (2014).

The radioactive content of the sediment, measured in $Bq.kg^{-1}$ and including $^{226}Ra$, $^{232}Th$, and $^{40}K$, varied between the 30 samples, with mean concentrations (±SD) of 60.7±21.3, 40.5±17.6, and 663±165, respectively; the ranges were from 30.4±2.1 (D-9.2) to 121.2±5.7 (D-7.3), 15.1±0.7 (D-9.2) to 86.6±3.2 (D-2.2), and 225±14 (D-9.2) to 1008±101 (D-8.1). On the other hand, 35, 30, and 400 ($Bq.kg^{-1}$) were reported as the global average radiation levels by UNSCEAR (2000). Global research, taking into consideration geochemical fluctuations, has shown that the average radioactive concentrations in freshwater basin sediments for $^{226}Ra$, $^{232}Th$, and $^{40}K$ are 31.8, 44.2, and 528 $Bq.kg^{-1}$, respectively (Faweya et al., 2013; Lu et al., 2008; Zhu & Shaw, 2000; El-Gamal et al., 2007; Suresh et al., 2011; Ramasamy et al., 2012; Qureshi et al., 2014; Krmar et al., 2009; Aközcan et al., 2018; Selçuk Zorer, 2019; Ali et al., 2019; Dentoni et al., 2020; Van et al., 2020; Duong et al., 2021; Isinkaye & Emelue, 2015). Table 5.1 shows that the Dharla River Basin (DRB)

had greater mean concentrations of $^{226}Ra$, $^{40}K$ and $^{232}Th$ than freshwater locations worldwide. As shown in Figure 5.1 (Khan et al., 2021) a comparative study with literature data selected from similar freshwater systems (lakes and rivers) with comparable geologies revealed that radioactivity levels in DRB deposits exceeded the published average levels.

Compared to freshwater basins, some coastal regions showed higher NORM quantities than those found in Dharla sediments. These regions included the sea beach in Orissa, India (Mohanty et al., 2004); the beach in Cox's Bazar, Bangladesh (Sasaki et al., 2014); Langkawi Island, Malaysia (Khandaker et al., 2018); the Atticocycladic beach, Greece (El-Gamal et al., 2007); and Milos Island, Greece (Florou et al., 2004). Furthermore, DRB's average 40K radiation levels were higher than those found in freshwater regions and coastal locations, with the exception of Lake Van Basin in Turkey (Selçuk Zorer, 2019) and the Teesta River in Bangladesh (El-Gamal et al., 2007) (Table 5.1).

## 5.2 Radiological Risk

Naturally occurring radionuclides can be hazardous to the public's and workers' health as well as different environmental components because of their chemotoxicity, radiotoxicity, and ionizing radiation (Habib et al., 2019). In order to evaluate the radiological hazards caused by NORMs in the Dharla river sediment, radiological indices such as $Ra_{eq}$ ($Bqkg^{-1}$), $H_{ex}$, $H_{in}$, $Ea_{ed}$ ($mSvy^{-1}$), D ($nGyh^{-1}$), Iγ, ELCR, and AUI are calculated and compared with pertinent literature data (Darwish et al., 2015; UNSCEAR, 2000, 2008; OECD, 1979), as shown in (Table 5.1).

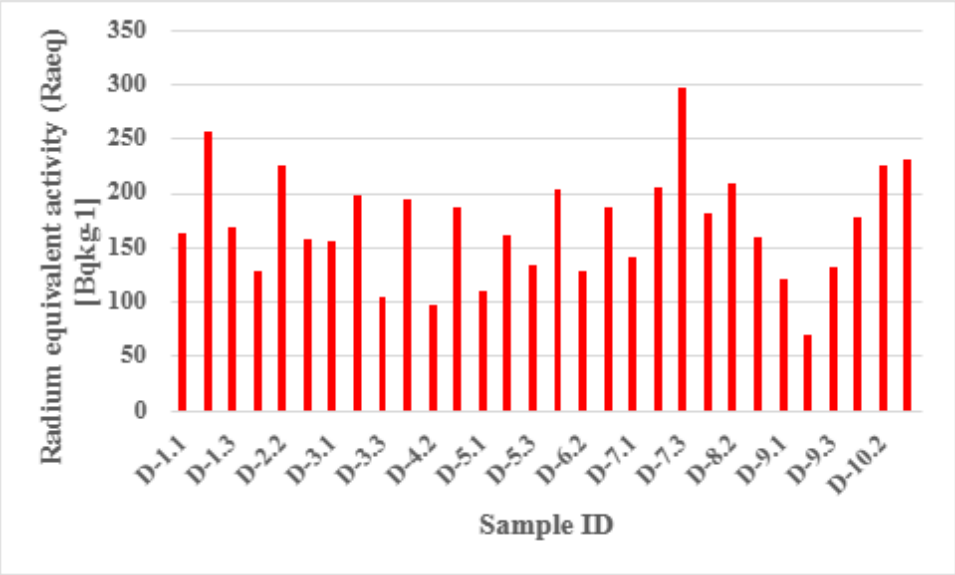


**Figure 5.1 Radium Equivalent Activity ($R_{aeq}$)**

$Ra_{eq}$ has an average value of 170 ± 59 $Bqkg^{-1}$, falling short of the required threshold of 370 Bq. $Kg^{-1}$ as per the OECD (1979), UNSCEAR (2008), and 2000. $Ra_{eq}$ varies from 69 to 296 $Bqkg^{-1}$. In comparison to other freshwater basins of similar size, $Ra_{eq}$ has a significantly higher average concentration (El-Gamal et al., 2007; Chowdhury et al., 1999; Krmar et al., 2009; Ramasamy et al., 2012; Isinkaye and Emelue, 2015; Zorer, 2019). Conversely, it is 2.55 to 10.5 times lower than the coastal regions (Table 5.1; Khandaker et al., 2018; Papadopoulos et al., 2016).

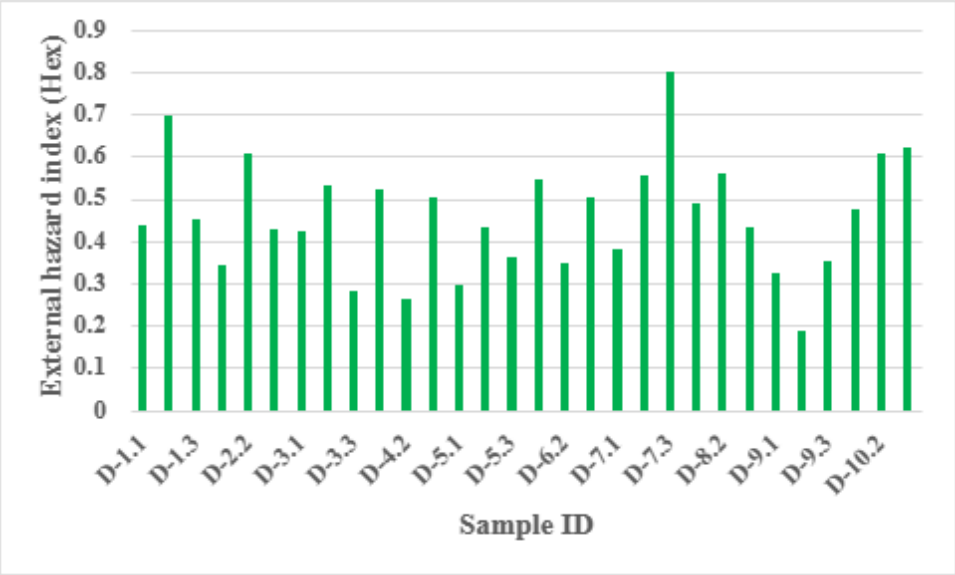


**Figure 5.2 External Hazard Index ($H_{ex}$)**

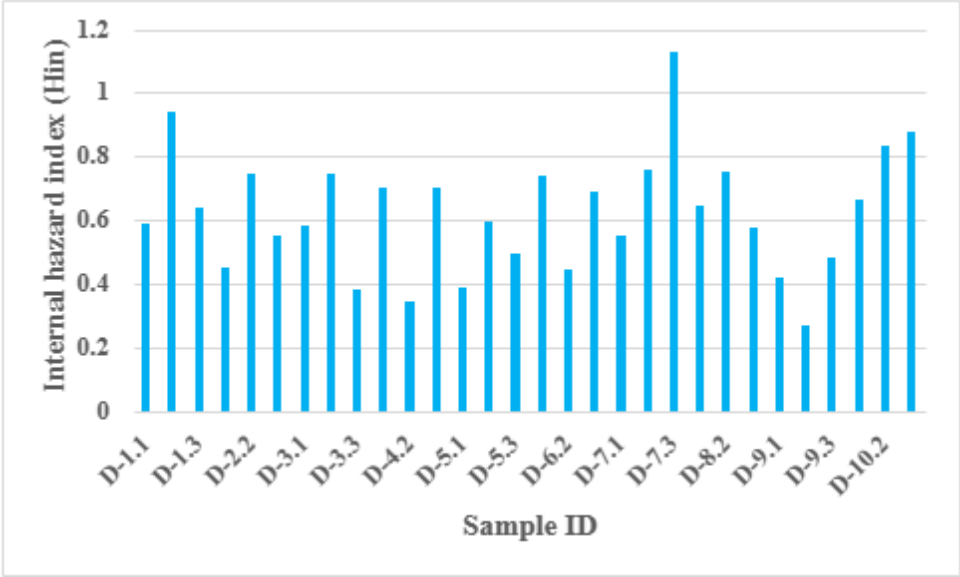


**Figure 5.3 Internal Hazard Index ($H_{in}$)**

The range of measurements for the internal and external hazard index is 0.27 to 1.13 (Figure 5.2) and 0.19 to 0.80 (Figure 5.3) respectively which is in average 0.46 to 0.62 and less than the required value but 1.2 to 6.5 times higher than those found in freshwater river basins worldwide. The required ranges of 0.36 to 1.51 and 0.45 to 1.98, respectively, are met by the average $H_{ex}$ and $H_{in}$ values of 0.46±0.16 and 0.62±0.22, respectively (Figure 5.1). Based on estimations of the

concentration of $H_{ex}$ and $H_{in}$, the Dharla river sediment may therefore represent a radioactive threat to the local population, who largely reside along riverbanks, as well as the aquatic ecosystem. It also endangers those who use this sand for construction purposes. As a result, the proper action needs to be taken.

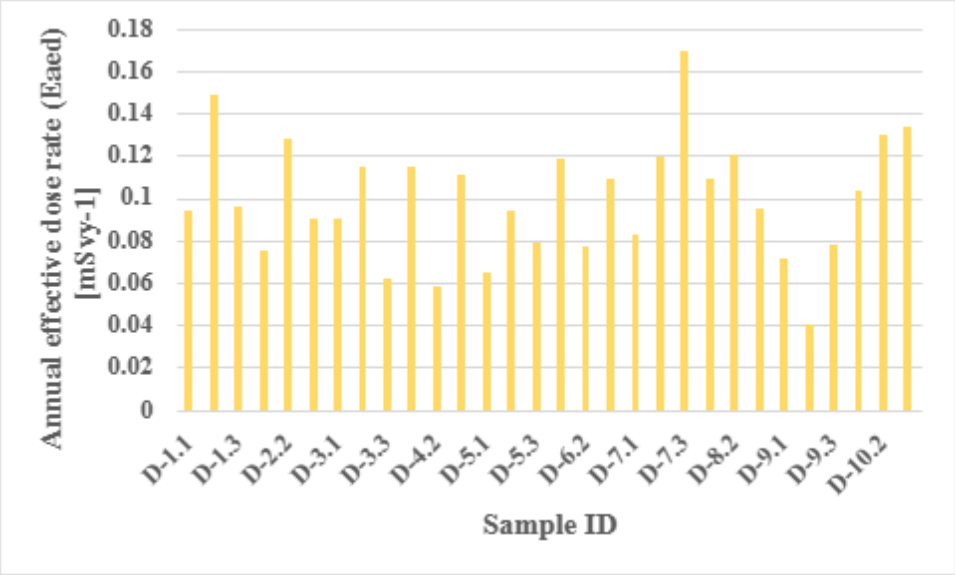


**Figure 5.4 Annual effective dose rate ($E_{aed}$)**

The mean value for $E_{aed}$ is 0.099 which is in line with the annual effective dose-rate requirement of 0.46 $mSvy^{-1}$ (OECD, 1979).

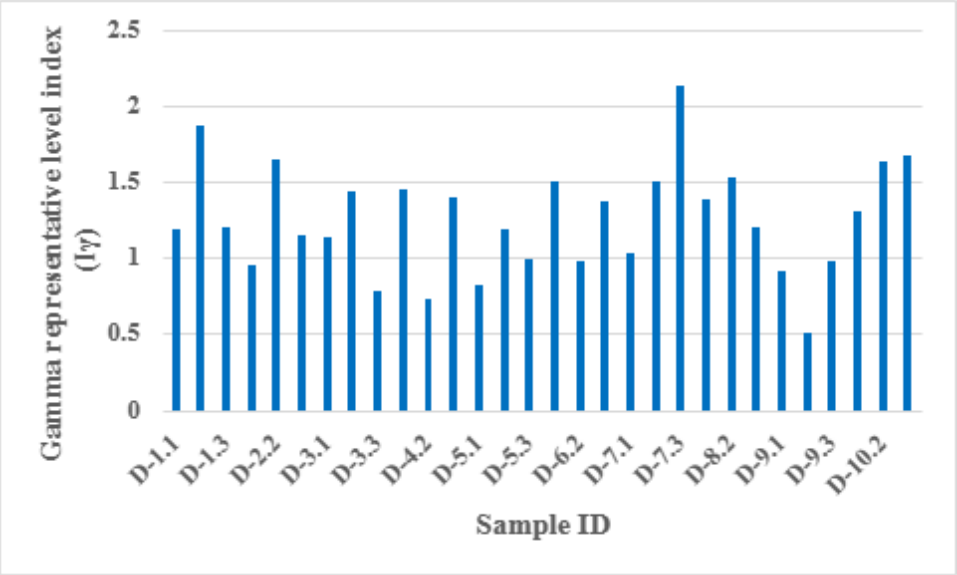


**Figure 5.5 Gamma representative level index (Iγ)**

The average $I_\gamma$ content is 1.25 times higher than the recommended value, indicating a higher radioactive threat from the Dharla River silt.

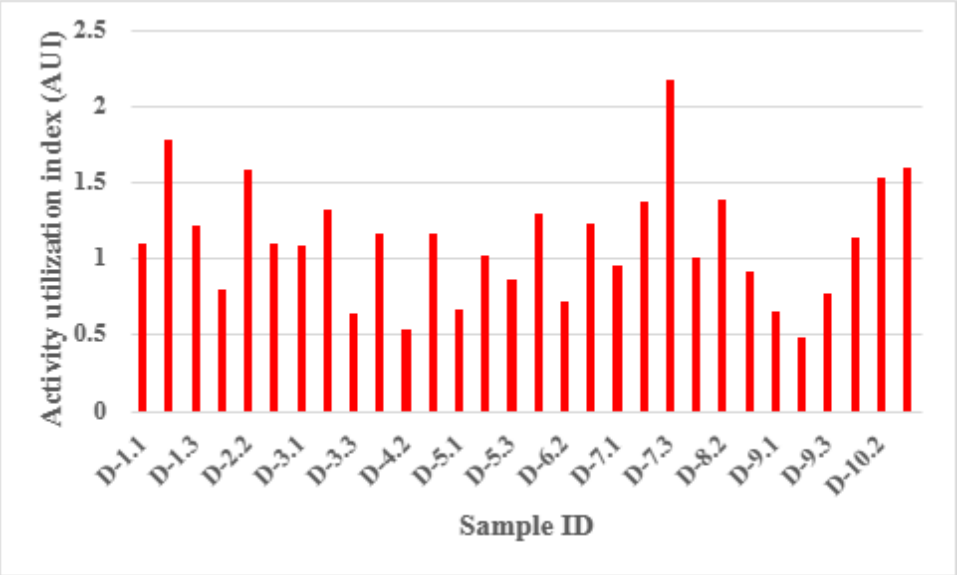


**Figure 5.6 Activity utilization index (AUI)**

Based on Darwish et al. (2015), the measured activity utilization index (AUI) shows that 2 sampling points are above the recommended limit, with an average value of 1.10 ± 0.42 and a range of 0.48 to 2.17. The mean AUI value is within the recommended limit. Lower AUI values (<2), however, imply that there might not be any significant problems using the Dharla river silt as a building material (Table 1).

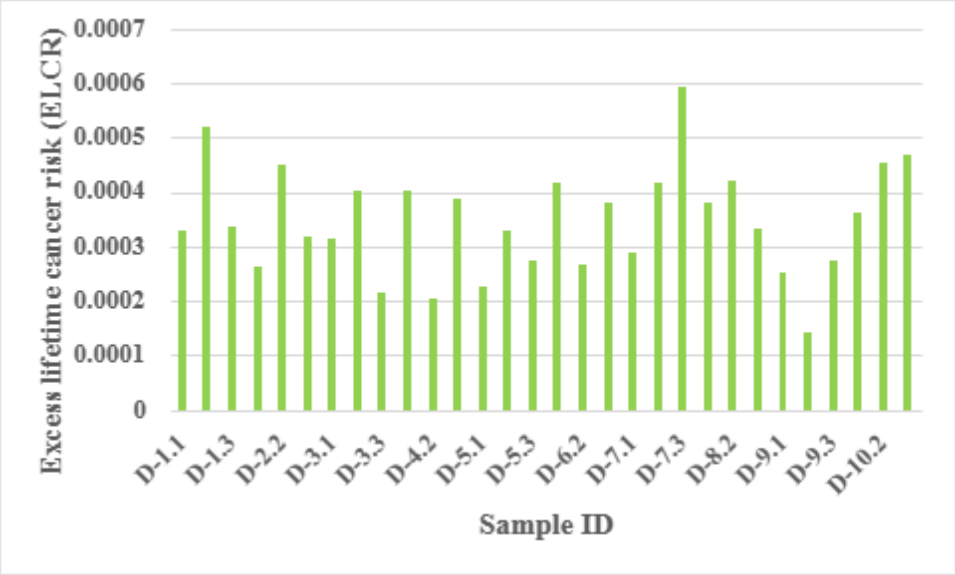


**Figure 5.7 Excess lifetime cancer risk (ELCR)**

The measured excess lifetime cancer risk (ELCR) values range from 1.41X10^04 to 5.94X10^04 due to naturally occurring radionuclides in the Dharla river sediment. The average value is 3.47X10^04 ± 1.19X10^04, significantly more than the recommended limit of 2.90×10-4 (UNSCEAR, 2000) (Table 5.1; Figure 5.7). The existence and enrichment of NORMs in the sediment from the Dharla riverbed that is used as building material can change the radiological properties of the surrounding area and possibly raise the concentration of naturally occurring radiation threats like ionizing radiation and continuously released gaseous $^{222}Rn$ ($^{222}Rn$: Taskin et al. 2009). When these radionuclides enter the human body through the food chain, they release different types of radioactive rays that might cause cancer, which can harm cell structures (Zorer 2019; Suresh et al. 2011).

Table 5.1 presents a comparison of the Dharla River's recorded radiological indices with those of other rivers in Bangladesh and freshwater basins across the globe. Compared to sediment from other freshwater basins in Bangladesh and around the world, the Dharla river silt has a higher radioactive risk. On the other hand, the greater concentration of heavy metals exclusively affects Bangladesh's coastal region and other global regions. Furthermore, compared to Bangladesh's coastal region, the dispersion of $^{40}K$ in the sediment of the Dharla river is more than seven times higher (Sasaki et al., 2014). The estimated radiological indices' relatively low concentration of $^{40}K$, when compared to the coastal region, indicates that the Dharla River's silt is less at risk from radiation (Table 5.1).

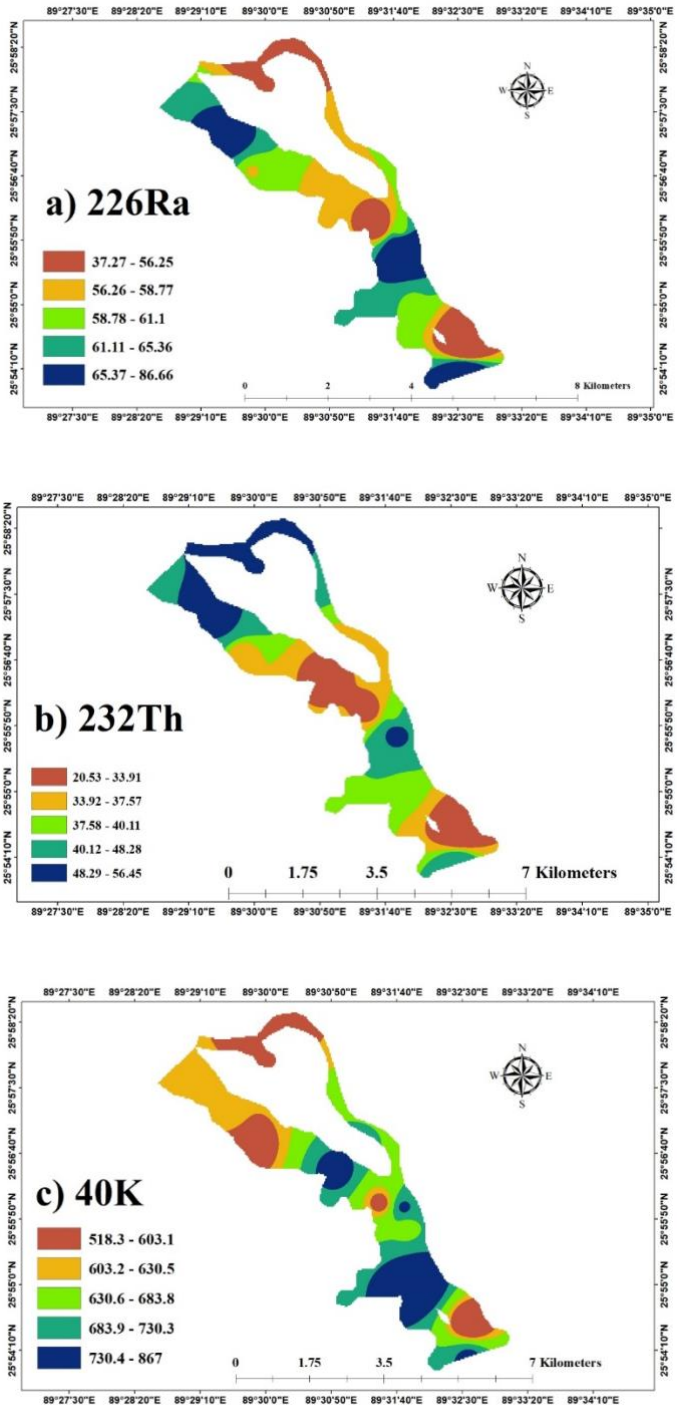


**Figure 5.8 Spatial distribution of radionuclides in the riverbed sediment of Dharla river.**

## 5.3 Policy Implications

The results of this study will help the Bangladeshi government and policymakers make well-informed decisions about projects in the Dharla river basin. It offers important details about naturally occurring radioactivity in the Dharla River sediment. Nevertheless, the following suggestions are made in light of the findings:

I. Install a system of continuous radio ecological monitoring for the Dharla river basin's vegetation, soil, water, air, and food. This should entail working with outside monitoring organizations and providing the necessary equipment.

II. Examine and revise current laws, rules, and directives:

a) Assure uniform radiation safety protocols across the region that comply with the most recent international guidelines.
b) Put into practice risk assessment techniques for biological, chemical, and radioactive contamination.

III. As part of a specialized project, carry out extensive impact research on hotspots that are currently and will soon be identified.

IV. Encourage scientific investigation that advances knowledge, assessment, and remediation of radiological problems in the Dharla River.

# Chapter 06

# Conclusion

The thorough evaluation of radioactive concentrations and radiological indices in the Dharla River sediments provide insightful information about the area's environmental radioactivity. Significant variations are seen in the measured activity concentrations of $^{40}K$, $^{232}Th$, and $^{226}Ra$ across sample locations; values at the direct discharge point are consistently lower than those at upstream and downstream sites. This trend is further highlighted by the Radium Equivalent Activity ($Ra_{eq}$), which shows possible human influences on activities related to Naturally Occurring Radioactive Materials (NORMs). In contrast to an increasing tendency in $^{40}K$ from upstream to downstream, the geographic distribution maps show larger concentrations of $^{226}Ra$ and $^{232}Th$ at upstream and downstream regions. The radiological indices that were computed, such as the Excess Lifetime Cancer Risk (ELCR), the Gamma Representative Level Index ($I_{\gamma}$), the Activity Utilisation Index (AUI), the Internal Hazard Index ($H_{in}$), the External Hazard Index ($H_{ex}$), the Absorbed Dose Rate (D), and the Annual Effective Dose Rate ($E_{aed}$), are all within the range of values that have been reported in comparable environmental studies. Overall, the results point to a complex interaction between human and natural variables affecting the distribution of radionuclides in the sediments of the Dharla River. The information provided here is extremely helpful in managing and monitoring the environment, as it helps to clarify the possible concerns related to radioactivity in this aquatic ecosystem. Still, more investigation and monitoring are needed to provide a more thorough evaluation of the long-term effects of human activity on the radiological profile of the river.

# Chapter 08

# References

Abedin, Md. J., & Khan, R. (2022). NORMs distribution in the dust samples from the educational institutions of Megacity Dhaka, Bangladesh: Radiological risk assessment. Journal of Hazardous Materials Advances, 8, 100155. https://doi.org/10.1016/j.hazadv.2022.100155

Ahad, A., ur Rehman, S., ur Rehman, S. and Faheem, M., (2004). Measurement of radioactivity in the soil of Bahawalpur division, Pakistan. Radiation Protection Dosimetry, 112(3), 443-447.

Ali, H., Khan, E., & Ilahi, I. (2019). Environmental Chemistry and Ecotoxicology of Hazardous Heavy Metals: Environmental Persistence, Toxicity, and Bioaccumulation. Journal of Chemistry, 2019, 1–14. https://doi.org/10.1155/2019/6730305

Ajayi, O.S. and Owolabi, T.P., (2007). Determination of natural radioactivity in drinking water in private dug wells in Akure, Southwestern Nigeria. Radiation protection dosimetry, 128(4), 477-484.

Azeem, U., Younis, H., ullah, N., Mehboob, K., Ajaz, M., Ali, M., Hidayat, A., & Muhammad, W. (2023). Radionuclide concentrations in agricultural soil and lifetime cancer risk due to gamma radioactivity in district Swabi, KPK, Pakistan. *Nuclear Engineering and Technology*. https://doi.org/10.1016/J.NET.2023.09.026

Bavarnegin, E., Moghaddam, M. V., & Fathabadi, N. (2013). Natural radionuclide and radiological assessment of building materials in high background radiation areas of Ramsar, Iran. *Journal of Medical Physics / Association of Medical Physicists of India*, *38*(2), 93. https://doi.org/10.4103/0971-6203.111325

Begum, M., Khan, R., Hossain, S. M., & Al Mamun, S. M. M. (2022). Redistributions of NORMs in and around a gas-field (Shabazpur, Bangladesh): radiological risks assessment. *Journal of Radioanalytical and Nuclear Chemistry*, *331*(1), 317–330. https://doi.org/10.1007/S10967-021-08107-X/METRICS

Boumala, D., Belafrites, A., Tedjani, A., Mavon, Ch., & Groetz, J.-E. (2019). Annual effective dose and excess life time cancer risk assessment from tobacco plants. *Perspectives in Science*, *12*, 100394. https://doi.org/10.1016/J.PISC.2019.100394

Chowdhury, M.I., Alam, M.N., Hazari, S.K.S., 1999. Distribution of radionuclides in the river sediments and coastal soils of Chittagong, Bangladesh and evaluation of the radiation hazard. Applied Radiation and Isotopes, 51, 747 - 755.,

Das, R., Islam, M.A., Naher, K., Khan, R., Tamim, U., Rashid, M.A., 2018. Distribution and Contamination of Trace Elements in Core Sediments of the Karnaphuli River using Neutron Activation Analysis. Nuclear Science and Applications, 27(2): 45-52.

Eker, Ç.S., Kiliç, E.D., 2018. Geochemistry of çoruh riverbed sediments in NE Turkey: implications in weathering-sedimentary cycle, provenance, and metal pollution. Geochem. Int. 56 (6), 579e600. https://doi.org/10.1134/ s0016702918060095.

El-Bahi, S.M., (2004). Assessment of radioactivity and radon exhalation rate in Egyptian cement. Health Phys. 86, 517-522.

EI-Gamal, A., Nasr, S., EI-Taher, A., 2007. Study of the spatial distribution of natural radioactivity in the upper Egypt Nile River sediments. Radiation Measurements 42, 457 – 465,

El, N.A., (2014). Studying of Naturally Occurring Radionuclides for Some Environmental Samples and Its Hazardous Effects (Doctoral dissertation, Fayoum University).

El Samad, O., Baydoun, R., Nsouli, B., & Darwish, T. (2013). Determination of natural and artificial radioactivity in soil at North Lebanon province. Journal of Environmental Radioactivity. http://dx.doi.org/10.1016/j.jenvrad.2013.02.010.

Faweya, E. B., Oniya, E. O., & Ojo, F. O., 2013. Assessment of Radiological Parameters and Heavy-Metal Contents of Sediment Samples from Lower Niger River, Nigeria. Arabian Journal for Science and Engineering, 38(7), 1903–1908. doi:10.1007/s13369-013-0549-6,

Florou, H., Kritidis, P., 1991. Natural radioactivity in environmental samples from an island of volcanic origin (Milos, Aegean Sea). Marine Pollution Bulletin 22 (8), 417e419.,

Gao, X., Chen, C.A., 2012. Heavy metal pollution status in surface sediments of the coastal Bohai Bay. Water Research, 46:1901-1911. https://doi.org/10.1016/j.watres.2012.01.007

Habib, M.A., Basuki, T., Miyashita, S., Bekelesi, W., Nakashima, S., Techato, K., Khan, R., Majlis, A.B.K. and Phoungthong, K., (2019). Assessment of natural radioactivity in coals and coal

combustion residues from a coal-based thermoelectric plant in Bangladesh: implications for radiological health hazards. Environmental monitoring and assessment, 191(1), 27.

Habib, M.A., Basuki, T., Miyashita, S., Bekelesi, W., Nakashima, S., Phoungthong, K., Khan, R., Rashid, M.B., Islam, A.R.M.T. and Techato, K., (2019). Distribution of naturally occurring radionuclides in soil around a coal-based power plant and their potential radiological risk assessment. Radiochimica Acta, 107(3), 243-259.

Habib, M. A., Islam, A. R. M. T., Bodrud-Doza, M., Mukta, F. A., Khan, R., Bakar Siddique, M. A., Phoungthong, K., & Techato, K. (2019). Simultaneous appraisals of pathway and probable health risk associated with trace metals contamination in groundwater from Barapukuria coal basin, Bangladesh. Chemosphere, 242. https://doi.org/10.1016/j.chemosphere.2019.125183.

Hameed, P.S., Pillai, G.S., Satheeshkumar, G. and Mathiyarasu, R., (2014). Measurement of gamma radiation from rocks used as building material in Tiruchirappalli district, Tamil Nadu, India. Journal of Radioanalytical and Nuclear Chemistry, 300(3), 1081-1088.

Hossain, A., Nizam, Q.M.R. and Rahman, M.M., (2014). Measurement of absorbed outdoor dose rate due to gamma radiation in northern part of Chittagong City Corporation. International Journal of Scientific & Technology Research, 3(5), 98-100.

Hossain, M. S., Khan, M. S. H., Chowdhury, K. R., & Abdullah, R. (2019). Synthesis of the tectonic and structural elements of the bengal basin and its surroundings. *Springer Geology*, 135–218. https://doi.org/10.1007/978-3-319-99341-6_6/COVER

IAEA, (2000). Progress Report on a Field Study of Soil-to-plant Transfer of Radioactive Caesium, Strontium and Zinc in Tropical Northern Australia. IAEA, Vienna, Austria.

Ibrahiem, N.M., Abd El Ghani, A.H., Shawky, S.M., Ashraf, E.M., Farouk, M.A., 1993. Measurement of radioactivity levels in soil in the Nile Delta and Middle Egypt. Health Physics 64 (6), 297-299.,

Isinkaye, M.O., Emelue, H. U., 2015. Natural radioactivity measurements and evaluation of radiological hazards in sediment of Oguta Lake, Southeast Nigeria. J o u rnal of Ra d i a t i o n Research and Ap p l i e d S c i e n c e s 8, 4 5 9-4 6 9.,

Islam, M. A., Al-mamun, A., Hossain, F., Quraishi, S. B., Naher, K., Khan, R., Das, S., Tamim, U., Hossain, S. M., & Nahid, F. (2017). Contamination and ecological risk assessment of trace elements in sediments of the rivers of Sundarban mangrove forest, Bangladesh. Marine Pollution Bulletin, 124(1), 356–366. https://doi.org/10.1016/j.marpolbul.2017.07.059

Islam, M.A., Das, B., Quraishi, S.B., Khan, R., Naher, K., Hossain, S.M., Latif, S.A., Hossen, M.B., 2020. Heavy metal contamination and their ecological risk assessment in water and sediments of the Halda river, Bangladesh: a natural fish breeding ground. Mar. Pollut. Bull. https://doi.org/10.1016/j.marpolbul.2020.111649

Islam, M.S., Ahmed, M.K., Raknuzzaman, M., Al-Mamun, M.H., and Islam, M.K., 2015. Heavy Metal Pollution in Surface Water and Sediment: A Preliminary Assessment of an Urban River in A Developing Country, Ecological Indicators, 48, 282–291.

Jibiri, N. N., & Okeyode, I. C. (2012). Evaluation of radiological hazards in the sediments of Ogun River, South-Western Nigeria. Radiation Physics and Chemistry, 81, 1829-1835.

Khalil, M.I., Majumder, R.K., Kabir, M.Z., Deeba, F., Khan, M.N.I., Ali, M.I., Paul, D., Haydar, M.A. and Islam, S.M.A., (2016). Assessment of natural radioactivity levels and identification of minerals in Brahmaputra (Jamuna) river sand and sediment, Bangladesh. Radiation Protection and Environment, 39(4), 204 (DOI: 10.4103/0972-0464.199980).

J. Beretka, & P. J. Mathew. (1985). *Natural Radioactivity of Australian Building Materials, Indu... : Health Physics*. National Institutes of Health. https://journals.lww.com/health-physics/abstract/1985/01000/natural_radioactivity_of_australian_building.7.aspx

Joel, E. S., Maxwell, O., Adewoyin, O. O., Olawole, O. C., Arijaje, T. E., Embong, Z., & Saeed, M. A. (2019). Investigation of natural environmental radioactivity concentration in soil of coastaline area of Ado-Odo/Ota Nigeria and its radiological implications. *Scientific Reports 2019 9:1*, *9*(1), 1–8. https://doi.org/10.1038/s41598-019-40884-0

Khan, R., Islam, H.M. T., Islam, A.R.M.T., 2021. Mechanism of elevated radioactivity in a freshwater basin: Radiochemical characterization, provenance and associated hazards. Chemosphere, (https://doi.org/10.1016/j.chemosphere.2020.128459),

Khan, R., Basir, M. S., Akhi, S. Z., Anik, A. H., Hossain, S., Islam, H. M. T., Islam, A. R. M. T., Idris, A. M., Khan, M. H. R., Aldawood, S., & Tareq, S. M. (2023). Radiation exposure and health concerns associated with the environmental geochemistry of relatively higher radioactivity in a fresh water basin. *Marine Pollution Bulletin*, *196*, 115588. https://doi.org/10.1016/J.MARPOLBUL.2023.115588

Khan, R., Islam, H. M. T., Apon, M. A. S., Islam, A. R. M. T., Habib, M. A., Phoungthong, K., Idris, A. M., & Techato, K. (2022c). Environmental geochemistry of higher radioactivity in a transboundary Himalayan river sediment (Brahmaputra, Bangladesh): potential radiation exposure and health risks. Environmental Science and Pollution Research, 29(38), 57357–57375. https://doi.org/10.1007/s11356-022-19735-5

Khan, R., Parvez, M. S., Tamim, U., Das, S., Islam, M. A., Naher, K., Khan, M. H. R., Nahid, F., Hossain, S. M., 2018. Assessment of rare earth elements, Th and U profile of a site for a potential coal based power plant by instrumental neutron activation analysis. Radiochim. Acta, 106(6), 515-524. https://doi.org/10.1515/ract-2017-2867

Khan, R., Shirai, N., & Ebihara, M. (2015). Chemical characteristic of R chondrites in the light of P, REEs, Th and U abundances. Earth and Planetary Science Letters, 422, 18–27. https://doi.org/10.1016/j.epsl.2015.04.008

Khandaker, M. U., Asaduzzaman, K., Sulaiman, A. F. B., Bradley, D. A., & Isinkaye, M. O., 2018. Elevated concentrations of naturally occurring radionuclides in heavy mineral-rich beach sands of Langkawi Island, Malaysia. Marine Pollution Bulletin, 127, 654–663. doi:10.1016/j.marpolbul.2017.12.055.

Kormoker, T., Proshad, R., Islam, S., Ahmed, S., Chandra, K., Uddin, M., Rahman, M., 2019. Toxic metals in agricultural soils near the industrial areas of Bangladesh: ecological and human health risk assessment. Toxin Reviews, 1135-1154.

Krmar, M., Slivka, J., Varga, E., Bikit, I., Vesković, M., 2009. Correlations of natural radionuclides in sediment from Danube. Journal of Geochemical Exploration 100, 20–24.,

Kumar, S., Islam, A.R.M.T., Hasanuzzaman, M., Salam, R., Islam, M.S., Khan, R., Rahman, M.S., Pal, S.C., Ali, M.M., Idris, A.M., Gustave, W., Elbeltagi, A., 2022. Potentially toxic elemental

contamination in Wainivesi River, Fiji impacted by gold-mining activities using chemometric tools and SOM analysis. Environmental Science and Pollution Research, https://doi.org/10.1007/s11356-022-18734-w

Lu, X., Zhang, X., & Wang, F., 2007. Natural radioactivity in sediment of Wei River, China. Environmental Geology, 53(7), 1475–1481. doi:10.1007/s00254-007-0756-0,

Maftei, A.E., Buzatu, A., Buzgar, N., Apopei, A.I., 2019. Spatial Distribution of Minor Elements in the Tazlău River Sediments: Source Identification and Evaluation of Ecological Risk. Int. J. Environ. Res. Public Health, 16:4664. https://doi.org/10.3390/ijerph16234664

Mbonu, C. C., & Ben, U. C. (2021). Assessment of radiation hazard indices due to natural radioactivity in soil samples from Orlu, Imo State, Nigeria. *Heliyon*, *7*(8), e07812. https://doi.org/10.1016/j.heliyon.2021.e07812

Mehra, R. and Singh, M., (2012). Estimation of radiological risk due to concentration of 238U, 226Ra, 232Th and 40K in soils of different geological origins in northern India.Turkish Journal of Physics, 36, 1-9.

Miah, F.K., Roy, S., Touchiduzzaman, M. and Alam, B., (1998). Distribution of radionuclides in soil samples in and around Dhaka city. Applied radiation and isotopes, 49(1-2), 133-137.

Milica, M.R., Nataša, B.S., Marija, M.J., Jelena, D.N., (2012). Radioactivity in chemical fertilizers. Institute for Nuclear Sciences "Vinča", University of Belgrade, Belgrade, Serbia

Mohanty, A. K., Sengupta, D., Das, S. K., Saha, S. K., & Van, K. V., 2004. Natural radioactivity and radiation exposure in the high background area at Chhatrapur beach placer deposit of Orissa, India. Journal of Environmental Radioactivity, 75(1), 15–33. doi:10.1016/j.jenvrad.2003.09.004

Ngachin, M., Garavaglia, M., Giovani, C., Njock, M.K. and Nourreddine, A., (2007). Assessment of natural radioactivity and associated radiation hazards in some Cameroonian building materials. Radiation Measurements, 42(1), 61-67.

Papadopoulos, A., Koroneos, A., Christofides, G., Papadopoulou, L., Tzifas, I., & Stoulos, S., 2016. Assessment of gamma radiation exposure of beach sands in highly touristic areas associated with plutonic rocks of the Atticocycladic zone (Greece). Journal of Environmental Radioactivity, 162-163, 235–243. doi:10.1016/j.jenvrad.2016.05.035

Papp, Z., (2010). Natural radioactivity in the soils of some eastern counties of Hungary. Radiation protection dosimetry, 141(1), 56-63.

Qureshi, A. A., Tariq, S., Din, K. U., Manzoor, S., Calligaris, C., & Waheed, A. (2014). Evaluation of excessive lifetime cancer risk due to natural radioactivity in the rivers sediments of Northern Pakistan. *Journal of Radiation Research and Applied Sciences*, *7*(4), 438–447. https://doi.org/10.1016/J.JRRAS.2014.07.008

Ramasamy, V., Paramasivam, K., Suresh, G., Jose, M.T., 2014. Role of sediment characteristics on natural radiation level of the Vaigai river sediment, Tamilnadu, India. Journal of Environmental Radioactivity 127, 64-74,

Ramasamy, V., Suresh, G., Rajkumar, P., Murugesan, S., Mullainathan, S., & Meenakshisundaram, V., 2011. Reassessment and comparison of natural radioactivity levels in relation to granulometric contents of recently excavated major river sediments. Journal of Radioanalytical and Nuclear Chemistry, 292(1), 381–393. doi:10.1007/s10967-011-1486-z ,

Rashed-Nizam, Q.M., Rahman, M.M., Kamal, M. and Chowdhury, M.I., (2014). Assessment of radionuclides in the soil of residential areas of the Chittagong metropolitan city, Bangladesh and evaluation of associated radiological risk. Journal of radiation research, 56(1), 22-29.

Rashid, M. U. (2022). *Bengal Delta: the definition, Boundaries and the Anthropogenic Aspects*. https://papers.ssrn.com/abstract=4560227

Sakib, K.N., (2015). Determination of Natural and Artificial Radionuclides in Soil Samples of Habigonj District, Bangladesh. Journal of Natural Sciences Research.

Sasaki, T., Rajib, M., Akiyoshi, M., Kobayashi, T., Takagi, I., Fujii, T., & Zaman, M. M., 2014. Laboratory Enrichment of Radioactive Assemblages and Estimation of Thorium and Uranium Radioactivity in Fractions Separated from Placer Sands in Southeast Bangladesh. Natural Resources Research, 24(2), 209–220. doi:10.1007/s11053-014-9248-6 ,

Selçuk Zorer, Ö. (2019). Evaluations of environmental hazard parameters of natural and some artificial radionuclides in river water and sediments. Microchemical Journal, 145, 762–766. https://doi.org/10.1016/j.microc.2018.11.035

Shetty, P. K., & Narayana, Y. (2010). Variation of radiation level and radionuclides enrichment in high background area. Journal of Environmental Radioactivity, 101, 1043-1047.

Shuaibu, H. K., Khandaker, M. U., Alrefae, T., & Bradley, D. A. (2017). Assessment of natural radioactivity and gamma-ray dose in monazite rich black Sand Beach of Penang Island, Malaysia. Marine Pollution Bulletin, 119(1), 423–428. https://doi.org/10.1016/j.marpolbul.2017.03.026

Siddiqui, E., Pandey, J., 2020. Assessment of heavy metal pollution in water and surface sediment and evaluation of ecological risks associated with sediment contamination in the Ganga River: a basin-scale study. Environ. Sci. Pollute. Res. 26 (11), 10926–10940. https://doi.org/10.1007/s11356-019-04495-6.

Stojanović, M., Stevanović, D., Milojković, J., Mihajlović, M.L., Lopičić, Z. and Šoštarić, T., (2012). Influence of soil type and physical–chemical properties on uranium sorption and bioavailability. Water, Air, & Soil Pollution, 223(1), 135- 144.

Suresh, G., Ramasamy, V., Meenakshisundaram, V., Venkatachalapathy, R., Ponnusamy, V., 2011. A relationship between the natural radioactivity and mineralogical composition of the Ponnaiyar river sediments, India. Journal of Environmental Radioactivity 102, 370-377,

Taskin, H., Karavus, M., Ay, P., Topuzoglu, A., Hindiroglu, S., & Karahan, G. (2009). Radionuclide concentrations in soil and lifetime cancer risk due to the gamma radioactivity in Kirklareli. Turkey Journal of Environmental Radioactivity, 100, 49-53.

Tufail, M. (2012). Radium equivalent activity in the light of UNSCEAR report. *Environmental Monitoring and Assessment*, *184*(9), 5663–5667. https://doi.org/10.1007/S10661-011-2370-6/TABLES/3

UNSCEAR (United Nations Scientific Committee on the Effects of Atomic Radiation). (2010). Sources, effects and risks of ionizing radiation. Annex B: exposures of the public and workers from various sources of radiation.

UNSCEAR, 2000. United Nations scientific committee on the effects of atomic radiation, 2000. In: Sources, Effects and Risks of Ionizing Radiation. Report to the General Assembly with Scientific Annexes. Annex-B, United Nations, NewYork.

UNSCEAR. (1993). Sources and effects of ionizing radiation. Report of the United Nations Scientific Committee on the Effects of Atomic Radiation to the general assembly. New York, USA: United Nations.

UNSCEAR. (2008). Report to the General Assembly, with annexes, v. 1, United Nations, New York

Usif, M.A.M. and El-Taher, A., (2008). Radiological assessment of Abu-Tartur phosphate, western desert Egypt. Radiation protection dosimetry, 130(2), 228- 235.

*Volcanos and Radioactivity on JSTOR*. (n.d.). Retrieved November 25, 2023, from https://www.jstor.org/stable/30056394

Warren, S. (n.d.). *How the Earth and moon formed, explained | University of Chicago News*. University of Chicago Press. Retrieved November 23, 2023, from https://news.uchicago.edu/explainer/formation-earth-and-moon-explained

Windsor, R. E., & Michaels, M. (2007). Radiation Safety – Theory and Practical Concerns. *Interventional Spine E-Book: An Algorithmic Approach*, 229–238. https://doi.org/10.1016/B978-0-7216-2872-1.50026-1

Zorer, Ö. S., 2019. Evaluations of environmental hazard parameters of natural and some artificial radionuclides in river water and sediments. Microchemical Journal. doi:10.1016/j.microc.2018.11.035 ,